

Progress and perspectives on phononic crystals

Cite as: J. Appl. Phys. 129, 160901 (2021); doi: 10.1063/5.0042337

Submitted: 29 December 2020 · Accepted: 1 April 2021 ·

Published Online: 22 April 2021



View Online



Export Citation



CrossMark

Thomas Vasileiadis,¹ Jeena Varghese,¹ Visnja Babacic,¹ Jordi Gomis-Bresco,² Daniel Navarro Urrios,² and Bartłomiej Graczykowski^{1,a)}

AFFILIATIONS

¹Faculty of Physics, Adam Mickiewicz University, Uniwersytetu Poznanskiego 2, 61-614 Poznań, Poland

²Departament de Física Aplicada, Universitat de Barcelona, IN2UB, Barcelona 08028, Spain

a)Author to whom correspondence should be addressed: bartłomiej.graczykowski@amu.edu.pl

ABSTRACT

Phononic crystals (PnCs) control the transport of sound and heat similar to the control of electric currents by semiconductors and metals or light by photonic crystals. Basic and applied research on PnCs spans the entire phononic spectrum, from seismic waves and audible sound to gigahertz phononics for telecommunications and thermal transport in the terahertz range. Here, we review the progress and applications of PnCs across their spectrum, and we offer some perspectives in view of the growing demand for vibrational isolation, fast signal processing, and miniaturization of devices. Current research on macroscopic low-frequency PnCs offers complete solutions from design and optimization to construction and characterization, e.g., sound insulators, seismic shields, and ultrasonic imaging devices. Hypersonic PnCs made of novel low-dimensional nanomaterials can be used to develop smaller microelectromechanical systems and faster wireless networks. The operational frequency, compactness, and efficiency of wireless communications can also increase using principles of optomechanics. In the terahertz range, PnCs can be used for efficient heat removal from electronic devices and for novel thermoelectrics. Finally, the introduction of topology in condensed matter physics has provided revolutionary designs of macroscopic sub-gigahertz PnCs, which can now be transferred to the gigahertz range with advanced nanofabrication techniques and momentum-resolved spectroscopy of acoustic phonons.

© 2021 Author(s). All article content, except where otherwise noted, is licensed under a Creative Commons Attribution (CC BY) license (<http://creativecommons.org/licenses/by/4.0/>). <https://doi.org/10.1063/5.0042337>

I. INTRODUCTION

In 1932, Frenkel¹ used the term phonon to describe a quantum of the acoustic field, a new hypothetical particle introduced 2 years earlier by Tamm.² The word phonon originates from Greek φωνή (phone, meaning voice), and it is an analogy to a photon being the quantum of the electromagnetic field. Needless to say that the importance of phonons in fundamental and applied research goes far beyond the common understanding of sound. The full phononic spectrum spans a broad, mostly inaudible, range of frequencies from a few millihertz up to dozens of terahertz. In general, the phononic spectrum (Fig. 1) consists of infrasounds (<few Hz), audible sound (from few Hz to 20 kHz), ultrasounds (from 20 kHz to 1 GHz), hypersounds (from 1 GHz to 1 THz), and heat (\gtrsim 1 THz at room temperature). For all these bands, acoustic waves/phonons are information and energy carriers that play an inherent role in condensed matter physics. The properties of the hosting medium dictate two fundamental features of phonons, i.e., their dispersion relation (spectral and spatial) and mean free path (lifetime and attenuation).^{3,4} For bulk, homogeneous solids, one

can distinguish three orthogonal modes (polarizations) of acoustic phonons: one (fast) longitudinal and two (slow) transverse phonons. At wavelengths much longer than the interatomic distances, all three modes are non-dispersive (phase and group velocities are independent of the momentum), typically up to hundreds of GHz. Hence, classical elastodynamics is sufficient to determine the phonon velocities.⁵

To alter the phonon propagation, one can employ spatial confinement and modulation of the material. The former approach turns bulk acoustic waves (BAWs) into surface acoustic waves (SAWs) propagating in close vicinity of free surfaces (Rayleigh, Sezawa, and Love waves) or Lamb waves in free-standing slabs and membranes.⁶ The second strategy was successfully realized in Phononic Crystals (PnCs), i.e., synthetic materials with periodic modulation of elastic properties utilizing the wave-like nature of phonons. The structure of PnCs mimics the arrangement of atoms in natural crystals and results in phononic features typical for thereof. These are the appearance of the second-order Brillouin zones, modification of the phonon dispersion, zone folding, and

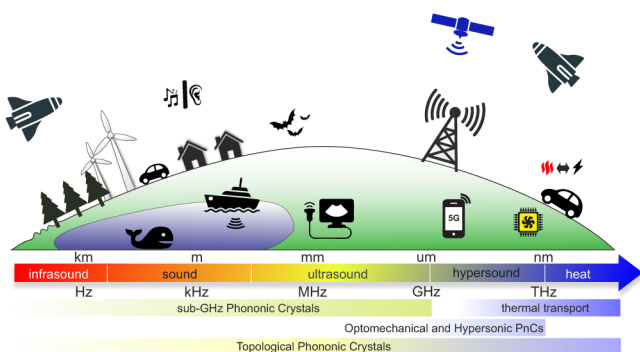


FIG. 1. The phononic spectrum—some natural and human-made sources of acoustic waves/phonons relevant for the considered applications of phononic crystals.

bandgaps due to Bragg reflections. In addition to Bragg gaps (BG), the so-called hybridization gaps (HGs) can appear when the periodic scatterers are made of mechanical resonators such as pillars, spheres, or stripes. The avoided crossing of the localized modes and propagating waves leads to sub- or super-wavelength stop bands robust to the PnC lattice imperfections.^{7–12} Generally, the position and width of the various types of bandgaps depend on the direction of motion of the acoustic wave inside the crystal.^{13–15}

The first theoretical proposals for 2D acoustic bandgap materials were published almost simultaneously by Sigalas and Economou¹⁶ and Kushwaha *et al.*¹⁷ Notably, one has to give credit to much earlier works from the 1970s and 1980s on the propagation of SAWs in periodically corrugated surfaces, being in fact 1D PnCs.^{18–20} In the last three decades, theoretical and experimental research on PnCs in the full phononic spectrum have flourished. Quite often, these studies were inspired by the achievements of the more mature fields of photonics and electronics. Nevertheless, the field of PnCs has introduced its original concepts employing the nature of phonons, their coupling with other elementary excitations, and their inseparable connection with the condensed matter.^{7–12,21}

This paper presents an experimentalists' point of view on the recent progress and prospects of PnCs. We present an overview of the advances in fabrication, experimental characterization, and new features for the broad spectrum of acoustic waves/phonons. The paper is organized as follows: first, we consider macroscopic PnCs aiming at the manipulation of sub-GHz waves (infrasound, sound, and ultrasound). Second, we focus on PnCs of a sub-micrometer feature size operating at GHz frequencies (hypersound). Third, we consider THz photon-GHz phonon coupling, both at sub-micrometer wavelengths, in periodic phononic-photon crystals (phoxonic, optomechanical crystals). Fourth, we discuss the role of THz phonons as the heat carrier in periodically modulated structures. Finally, we cover recent advances and prospects of topological phononics in a broad spectrum of frequencies.

II. SUB-GIGAHERTZ PHONONIC CRYSTALS

Since the earlier works on sonic bandgap crystals,^{22,23} research on PnCs and acoustic metamaterials (AMMs) in the sub-GHz

frequency spectrum is an active domain with promising applications. First, the technological advances in additive manufacturing (3D printing) offered a great solution to transfer many intricate theoretical designs into laboratory-scale structures. The challenges of practical applications can be resolved with auxetic metamaterials, acoustic metasurfaces, and tunable and multifunctional AMMs. In particular, widening the locally resonant bandgaps of periodic structures can improve the performance of seismic shields, ultrasonic waveguides, and other phononic devices. Sub-GHz phononics need a heterogeneous community to bring together the concepts of several scientific disciplines: device physics, geology, mathematics, civil engineering, electronics, and telecommunications, to name a few. Here, we address the possible directions of phononic materials research for manipulating seismic waves, sound, and ultrasonic waves with the feature size ranging from a few meters to micrometer scale, respectively. Theoretical PnC designs are out of the scope of this Perspective, and a detailed review on PnCs and AMMs can be found in other articles.^{4,24–29}

A. From infrasonic to ultrasonic designs

The practical size limitation of PnCs is enough to motivate locally resonant structures for ultra-low frequency applications. However, functional sub-wavelength scale PnCs need improvement regarding compactness, weight, and cost effectiveness. For example, a metabarrier consisting of few-meter-sized resonant structures (cylindrical mass in concrete slabs)³⁰ can convert the seismic Rayleigh surface waves (RSWs) to shear BAWs that attenuate on the soil surface. Such locally resonant structures are widely used as seismic shields/insulators^{30–32} in the configurations like inclusions in the soil^{31,33} or buried mass resonators.^{34,35} Interestingly, AMMs are not strictly artificial. A forest of trees can act as a natural PnC^{36–38} [Fig. 2(a)] and offers large attenuation of seismic RSWs and shear waves (S-waves) in the broad frequency range below 150 Hz [Fig. 2(b)]. Graded vertical pillars arranged on an elastic substrate can block RSWs by reflecting them (classical wedge showing rainbow effect) or by converting them to BAWs (inverse wedge).³⁹ These experiments have to be realized in the geological scale, and they involve designing tree wedges with height varying profiles and artificial vertical pillars for seismic protection. However, the potential of each design depends on the geometry of the structure and the viscoelastic properties of the soil.³⁴ While numerous theoretical models^{24,34,49–51} of phononic structures in various geometries and dimensions are available, the experimental realization is still challenging. Fabrication methods experience several limitations in terms of low-cost raw material choice, minimum feature size, aspect ratios, or support requirements.⁵² Additive manufacturing technologies, including stereolithography, material jet printing, fused deposition modeling, and microlaser sintering/melting, make the design of 3D sonic PnCs much more feasible in the millimeter scale.^{52–55} Rainbow metamaterials are one of the best examples of structures with broad and robust sonic bandgaps.⁵⁶ Such systems with lightweight structures were first observed in the context of optical waves⁵⁷ and were further expanded to realize their acoustic analogs. Chen *et al.*⁵⁸ have designed a gradient metamaterial beam for the enhancement of flexural waves. Disorder induced bandgap tuning has been studied using a 3D

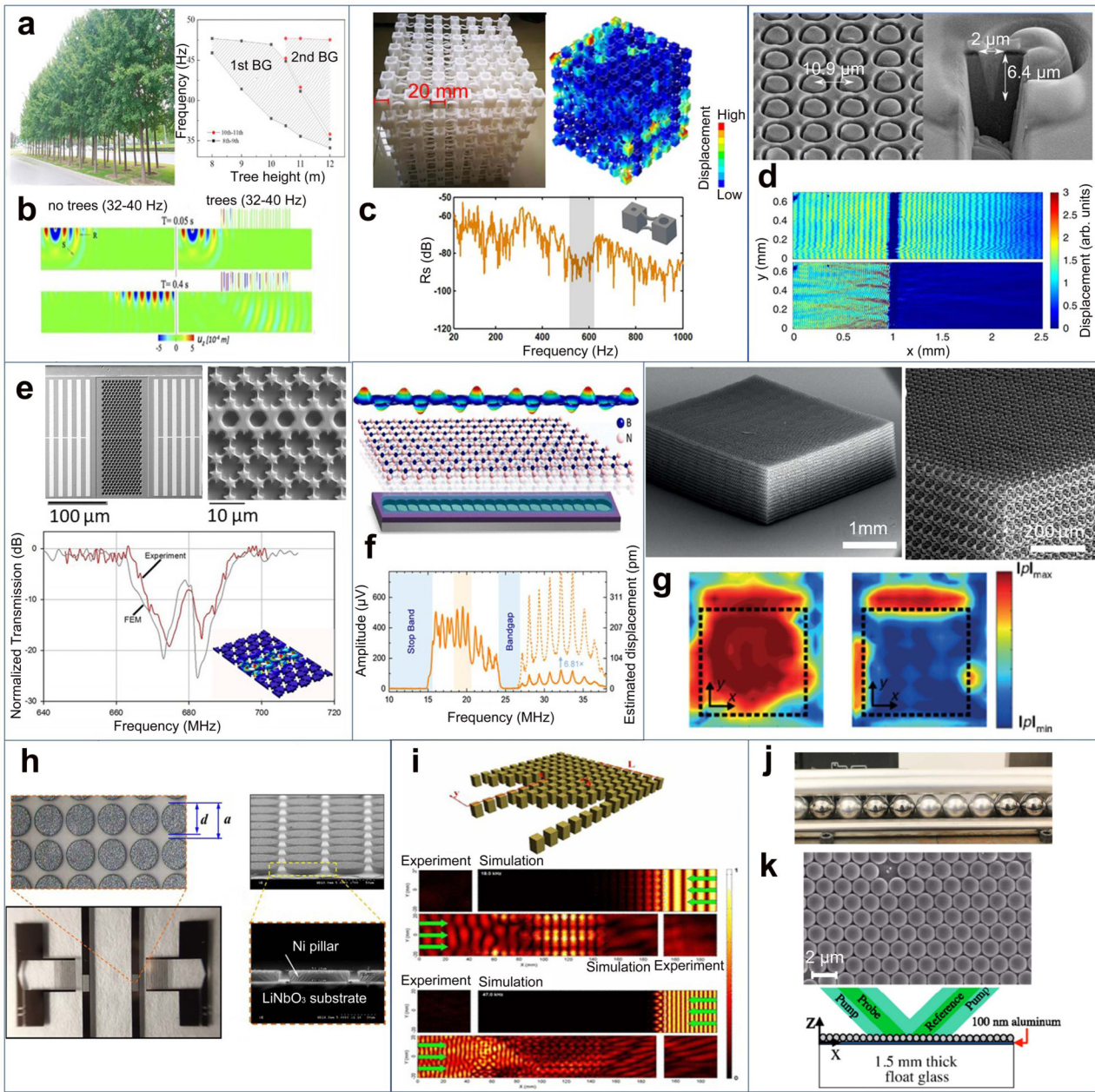


FIG. 2. Sub-GHz phononic materials: (a) natural PnC made of trees³⁸ and (b) filtering of seismic Rayleigh and S-waves.³⁶ (c) 3D sonic rainbow metamaterial⁴⁰ and (d) annular hole PnC.⁴¹ Waveguides made of (e) SiC-air PnC in a hexagonal lattice,⁴² (f) h-BN coupled resonator arrays,⁴³ and (g) microlattice for ultrasonic transmission.⁴⁴ Pillar PnC arrays for (h) acoustofluidics⁴⁵ and (i) acoustic diode.⁴⁶ Tunable granular crystals: (j) macroscopic bead array of steel–aluminum spheres of millimeter size⁴⁷ and (k) self-assembled 2D layer of polystyrene particles of 1 μm diameter and the schematic of the pump–probe experimental setup to probe the interactions between spherical particles contact resonances and propagating SAWs.⁴⁸ (a)–(k) Reproduced with permissions from Colombi *et al.*, Sci. Rep. **6**, 19238 (2016). Copyright 2016 Springer Nature; Huang *et al.*, Int. Soil Water Conserv. Res. **7**, 196 (2019). Copyright 2019 Elsevier Ltd./iswcr; Meng *et al.*, Sci. Rep. **10**, 18989 (2020). Copyright 2020 Springer Nature; Ash *et al.*, Nat. Commun. **8**, 174 (2017). Copyright 2017 Springer Nature; Ghasemi Baboly *et al.*, Appl. Phys. Lett. **112**, 103504 (2018). Copyright 2018 AIP Publishing LLC; Wang *et al.*, ACS Photonics **6**, 3225–3232 (2019). Copyright 2019 American Chemical Society; Krödel and Daraio, Phys. Rev. Appl. **6**, 064005 (2016). Copyright 2016 American Physical Society; Hsu and Lin, Sens. Actuators A **300**, 111651 (2019). Copyright 2019 Elsevier Ltd.; Li *et al.*, Phys. Rev. Lett. **106**, 084301 (2011). Copyright 2011 American Physical Society; Kim and Yang, Funct. Compos. Struct. **1**, 012002 (2019). Copyright 2019 IOP Publishing; and Vega-Flick *et al.*, Phys. Rev. B **96**, 024303 (2017). Copyright 2017 American Physical Society.

printed cantilever-in-mass design showing the wave trapping effect.⁵⁴ This study revealed that mistuning in the design of the metamaterial can destroy its bandgaps. In some cases, irregularities in the design of PnCs can lead to wider bandgaps. For sonic rainbow PnCs [Fig. 2(c)], a nearly periodic system of cuboids connected by curved beams shows an attenuation bandwidth twice that of the periodic design of equal mass.⁵⁹ Although 3D printing methods have revolutionized microscale structures with complex geometries, a large scale production strategy at low cost is still under development. 4D printing methods are the next game-changer, which may accelerate the scaling-up procedure from laboratory prototypes to large-scale devices.⁶⁰ In addition, artificial intelligence (AI) based techniques, like topological optimization and machine learning, may lead to improved design methodologies.^{61–63}

Recently, soft AMMs were introduced to manipulate ultrasonic waves for applications like sub-wavelength imaging, acoustic lenses, and transformation acoustics.^{64,65} The design is based on sub-wavelength resonators suspended in an acoustic fluid. Such “soft-gel nature” offers a feasible step towards tunable and responsive AMMs that allows molding the metamaterial in the desired shape, size, and dimensions. 3D ultrasonic metafluid with macroporous microbeads fabricated by soft matter techniques exhibited double negative acoustic impedances. The silicon rubber beads of mean radius 160 μm suspended in the water-based gel matrix act as Mie resonators showing strong monopolar and dipolar resonances. This approach can be exploited on large scale to produce zero or negative index materials for acoustic imaging applications.^{25,27,66,67}

Hierarchical architectures have been used to improve structural integrity and to minimize the amount of material. Several works have explored how the unit cell geometries, lattice material, and dimensions can tailor the phononic properties.^{68–70} A 3D microlattice [Fig. 2(g)] made by 2-photon lithography can exploit the ultrasonic wave propagation in water by elastoacoustic hybridization. The lattice design with truss-like elements (lattice constant about 70 μm) allows tailoring the HG that effectively attenuates the acoustic waves due to fluid interaction. A very high transmission (>80%) in the high frequency ultrasonic range (nearly 30 MHz) is observed outside this bandgap due to the impedance matching with that of water. This can be further used in biomedical imaging, where smaller penetration depth and higher resolution are important.⁴⁴ These microlattices are scalable and can find use as resonators, acoustic insulators, and ultrasonic transducers.⁷¹

Micro-electro-mechanical systems (MEMS) harnessing RF SAWs are important for signal processing and telecommunications.⁷⁶ A standard design of SAW devices is a periodic array of etched holes.⁷⁷ However, the bandgaps of such systems lie in the frequency range of leaky SAWs. In that sense, locally resonant (LR) structures in composite pillar arrays were used to open low-frequency LR bandgaps for SAW propagation.⁷⁸ A finite depth annular hole PnC⁴¹ [Fig. 2(c)] analogous to the pillared architecture revealed potentially improved LR bandgaps. The uniform array of holes was fabricated in a lithium niobate (LiNbO_3) delay line using focused ion beam (FIB) etching. Moreover, the SAW attenuation has additional geometric freedom compared to the cylindrical pillar designs allowing tailorabile SAW dispersions. This design can be exploited where strong acoustic confinement and miniaturization are indispensable. For example, a pillar PnC device [Fig. 2(h)]

made of nickel pillars electroplated on the LiNbO_3 substrate achieved perfect scattering of standing SAWs (nearly 30 MHz). This generated strong acoustic radiation force and was exploited for concentrating and separating polystyrene microparticles.⁴⁵ The annular hole PnC design can be exploited in SAW devices for microfluidics^{79–81} and further extended to different particle size combinations and biomolecules.

The introduction of defect modes in a periodic crystal can trap the acoustic energy. For example, inserting space gaps in a square array of cylindrical pillars improves the performance of demultiplexing and wave filtering.⁸² A 2D SiC-air PnC with circular inclusions produced waveguiding at 680 MHz allowing 39% transmission of the acoustic energy [Fig. 2(e)].⁴² Comparison of 90° bend and straight waveguides showed that curved paths produce additional losses.⁸³ A coupled-resonator array [Fig. 2(f)] using hexagonal boron nitride PnC (fabricated by the integrative approach of dry exfoliation after FIB etching and patterning) supported the MHz wave propagation over an effective distance of 1.2 mm.⁴³ The piezoelectric properties of this crystal, and van der Waals layered materials, can be explored further to generate tunable devices for RF applications. Recently, a virtual soft boundary based AMM design with resonant tube arrays allowed frequency separation keeping the flow of the medium unaffected.⁸⁴ This method can be further explored to design complex functional waveguides and is also viable for microfluidic applications in the future. Waveguides suffer signal losses; future phononic devices have a significant role in achieving better confinement.

B. Tunable and active phononic structures

Granular crystals, ordered macroscopic beads [Fig. 2(j)] interacting via adhesion forces exhibited interesting wave propagation characteristics.^{85,86} From the experimental verification of “sonic vacuum,”^{48,87} these crystals demonstrated non-linear waves (solitons) with strong localization, discrete breathers,⁸⁸ rotational elastic wave propagation,⁸⁹ and several engineering applications as tunable wave filters, acoustic lenses, switches, and rectifiers.^{90,91} The flexibility in terms of size, shape, stiffness, and spatial orientation of solid particles in the lattice makes them easily tailorable for acoustic phenomena. In addition, tunability in terms of precompression transformed the wave propagation from a highly non-linear regime (with no compression) to a nearly linear regime (with precompression).

Self-assembling has enabled scaling down granular crystals to micrometer feature size large area/volume structures. In such systems [example in Fig. 2(k)], laser pump-probe experiments (transient grating technique) revealed a critical role of inter-particle and particle–substrate bonding due to adhesion in forming acoustic bandgaps for SAWs and Lamb waves.^{92,93} Notably, even disordered 2D granular crystals could effectively attenuate SAWs near their resonant frequency, serving as a perfect metamaterial for wave attenuation and filtering.⁹⁴ Compared with commonly used pillar resonant structures, microgranular crystals are weakly adhered to the substrate. In this Perspective, the resonant frequency can be tailored by the inter-particle and particle–substrate contacts via temperature or hydrostatic pressure treatments below the glass transition temperature.^{95,96} A complex contact dynamics of SAW

attenuation was explained by Hiraiwa for tailored microspheres using scanned laser ultrasonics.⁹⁷ The interparticle stiffness was modified via the deposition of a thin aluminum film over the monolayer, ultimately exhibiting horizontal-rotational contact resonances in addition to vertical resonances. This improved the attenuation regime opening additional bandgap at the lower resonances. Recently, splitting of the spheroidal contact resonance resulting from the symmetry breaking of the substrate was explained.⁴⁸ These studies can lead to engineering of SAWs devices such as filters, sensors, and waveguides. In addition, advances in self-assembly enable scaling down to nanosphere dimensions, opening a broad horizon to manipulate wave propagation in the hypersonic regime (see Sec. III).

An important aspect of phononic materials, which broadens their potential applications, is tunability. Some examples are self-modulated metamaterials,^{98–100} Helmholtz resonators,¹⁰¹ membranes,^{102,103} fluid-filled hollow pillars (whispering gallery modes),¹⁰⁴ split ring resonators,¹⁰⁵ piezoelectric materials,^{106,107} decorated membrane resonators (DMRs),¹⁰⁸ and electromagnetic field controls.^{109,110} Some studies have also focused on flexible origami and kirigami-inspired cut and folded metamaterials⁷³ [Figs. 3(a)–3(c)]. A waveguide¹¹¹ designed for audible frequency proposed a broad working band and switchable sound propagation. Pentamode metamaterials [Fig. 3(d)] having their rigidity maintained about the point contacts of elongated unit cells show that their bulk and shear nature is essentially decoupled.^{75,112} Several of such designs can be proposed by virtue of their richness in deformation modes. We also envision that bioinspired and natural PnCs and AMMs will become a more intensive field of study. Overall, the future of sub-GHz phononics is vested in active and reconfigurable structures.

III. HYPERSONIC PHONONIC CRYSTALS

The frequency of 1 GHz is the conventional boundary between ultrasounds and hypersounds that can also be assumed in the description of PnCs. Due to their small feature size, which is typically less than 1 μm , the fabrication, experimental characterization, and applications of hypersonic PnCs differ significantly from those of sub-GHz PnCs. Hypersonic PnCs can be potentially useful for the development of high-frequency signal processing devices for wireless communications. Nowadays, the operational frequency of wireless communications is in the order of 1 GHz. The future front-end modules have to manage signals from a few to hundreds of GHz to reach the requirements of the next-generation wireless networks. For this purpose, hypersonic PnCs can be implemented as BAW, SAW, and Lamb waves filters, according to their architecture.

A. Hypersonic phononic crystals in various dimensions

Three-dimensional (3D) hypersonic PnCs allow tailoring of BAWs dispersion employing Bragg reflections and local resonances similarly to sub-GHz PnCs. To date, a vast variety of 3D PnCs were fabricated employing self-assembling of monodispersed sub-micrometer particles into colloidal crystals (CCs). As in the case of sub-GHz PnCs, the key advantages of CCs are their large volume, low cost, and low-effort fabrication, maintaining a

high-quality translational order. Also, the forbidden range of frequencies can be adjusted by the NPs size and material and the material of the matrix.

The first experimental observation of GHz bandgaps was reported by Cheng *et al.*¹¹⁶ in solid/liquid PnCs. The structures were made of polystyrene (PS) nanoparticles (NPs) self-assembled into face-centered-cubic (fcc) CCs and infiltrated with various fluids. Notably, the observed BG (at about 5 GHz) offered some degree of tunability by the NPs size and the infiltrated fluid type. Figure 4(a) displays an example of a solid/solid PnC that was fabricated from self-assembled PS NPs embedded in the polydimethylsiloxane (PDMS) matrix.¹¹⁷ The band diagram and transmission spectrum calculated for this material revealed both BG and HG. However, the experimental data confirmed only the former type centered at about 4 GHz. In addition to the geometry and material parameters, the phononic dispersion of CC PnCs can be tailored by bondings between the NPs. This effect and filtering due to the local resonances were reported for CCs made of silica NPs.¹¹⁸ For this material, femtosecond pump-probe technique revealed a long-living mode at 7.5 GHz matching the center of the calculated bandgap. It was demonstrated that the sintering of silica NPs could modify this stop band.

The reduction of CC's symmetry results in higher acoustic anisotropy of PnCs. This effect was observed for CCs fabricated from non-spherical NPs, i.e., nanoellipsoids depicted in Fig. 4(b). In such PnCs, the phononic dispersion [Fig. 4(b)] can be tuned by changing the NP's aspect ratio, which leads to unidirectional HG.¹¹⁹ The symmetry reduction of PnCs was also achieved by directional deformation of flexible solid/solid CCs. This was demonstrated for PS-PDMS CCs stretched along the [1̄1̄] direction. In this case, the unidirectional expansion of about 17% resulted in the redshift of the BG. Notably, HGs were found as practically resilient to structural changes.¹²⁷ This effect can be utilized in flexible devices that require the performance of PnCs robust to large deformations. In a more general context, HGs are independent of the PnCs' structural imperfections. A recent study has demonstrated a new approach for tunability of HGs in hybrid organic/inorganic PnCs through a complex structure of spherical NPs. The PnCs were composed of self-assembled PS brush-grafted silica NPs with elastic anisotropy across the silica core–polymer shell interface. The spectral position of HGs was adjusted within 5.5–10 GHz range by the degree of polymerization, grafting density, and NP core size [Fig. 4(c)].¹²⁰

Two-dimensional (2D) hypersonic PnCs have been utilized for altering the propagation of different types of SAWs or Lamb waves. Such systems were designed as 2D periodic patterns on the free surface of bulk or membrane and fabricated employing the bottom-up or top-down approach. The former method is based on large-area 2D CC, i.e., self-assembling of NPs into close-packed monolayers. Figure 4(d) displays 2D PnCs composed of a PS NPs monolayer deposited on a 50 nm thick Si_3N_4 membrane.¹²¹ For these systems, the measured and calculated phononic dispersion pointed to three distinct types of bandgaps for Lamb waves. Namely, they were related to the lattice period (BG), NP–membrane contact resonance (HG), and local resonances of NPs (HG). Notably, the latter type was found to appear in the sub-wavelength (below BG) and super-wavelength (above BG) regimes. The central

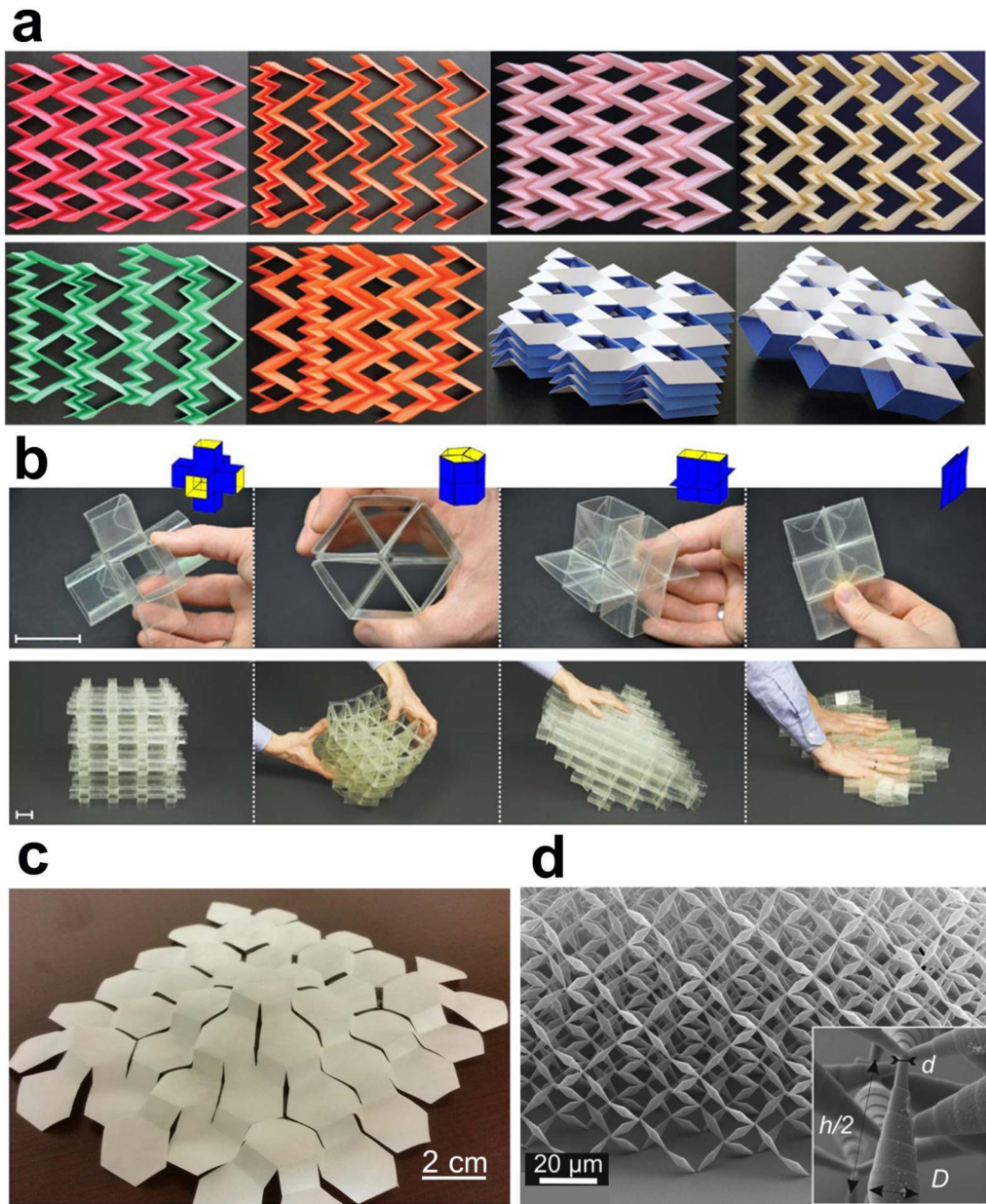


FIG. 3. Reconfigurable metamaterials: origami-inspired metamaterial designs. (a) Unit cells with holes arranged in layers,⁷² (b) mechanical MMs with cubic microstructures,⁷³ (c) combining cut fold structures in 2D sheets,⁷⁴ and (d) pentamode metamaterial⁷⁵ design by 3D DLW optical lithography. (a)–(d) Reproduced with permissions from Eidini and Paulino, *Sci. Adv.* 1, e1500224 (2015). Copyright 2015 AAAS Publishing; Overvelde *et al.*, *Nat. Commun.* 7, 10929 (2016). Copyright 2016 Springer Nature; Sussman *et al.*, *Proc. Natl. Acad. Sci. U.S.A.* 112, 7449–7453 (2015). Copyright 2015 PNAS; and Kadic *et al.*, *Appl. Phys. Lett.* 100, 191901 (2012). Copyright 2012 AIP Publishing LLC.

frequencies of all three types of bandgaps can be tuned by the particle size, membrane thickness, and adhesion at the NP–NP and NP–membrane interfaces.

The top-down fabrication requires more effort as typically it is based on electron beam lithography (EBL) and reactive ion etching

(RIE).¹²⁸ Here, one can distinguish two types of PnCs: solid/air and solid/solid differing in the periodic motifs. The former is realized by the substrate perforation (holes), while the latter by the periodic mass loading (pillars). Both of these schemes were exploited in the PnCs dedicated to the SAWs management.^{123,129–132} In this case,

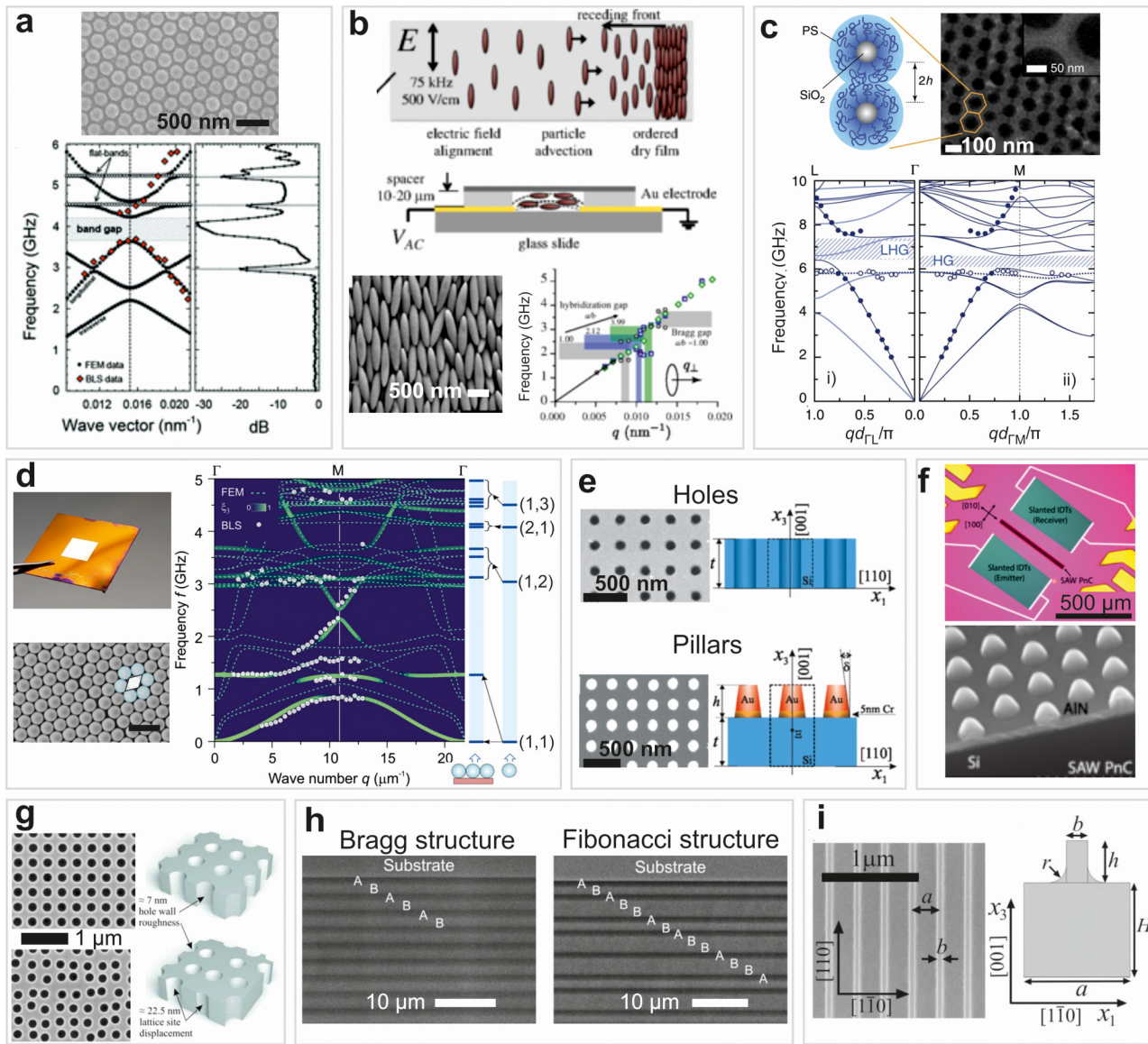


FIG. 4. (a) 3D PnC made of PS spheres embedded in solid PDMS matrix and corresponding band structure.¹¹⁷ (b) 3D PnC realized of carboxylate modified PS nanoellipsoids. Phononic band diagrams for the q_{\perp} propagation directions when $\alpha/b = 2.12$ (blue squares), $\alpha/b = 3.99$ (green diamonds), and for $\alpha/b = 1$ (black circles).¹¹⁹ (c) PS brush-grafted silica NPs assembly; dispersion calculated along (i) [111] shows non-degenerate longitudinal (dark solid lines), double degenerate transverse (light solid lines), and deaf bands (dotted lines); (ii) [112] shows non-degenerate of mixed character and the flatband. Hybridization gaps LHG (for longitudinal modes) and HG (for all modes) are indicated with shaded areas.¹²⁰ (d) 2D PnC composed of single layer PS nanoparticles self-assembled on a thin Si_3N_4 membrane and related dispersion relation.¹²¹ (e) Solid-air and solid-solid 2D PnC fabricated by making a pattern of holes and pillars in/on a thin Si membrane, respectively.¹²² (f) Optical image of the device showing a ribbon of the SAW PnC between emitter and receiver (top). SEM image of the cross section of 2D pillar-based SAW-PnC structure (bottom).¹²³ (g) SEM images of 2D PnC with ordered (top) and disordered pattern of holes (bottom) in Si membrane.¹²⁴ (h) Bragg structure made of periodically altering layers of Si with different porosity (left) and quasi-periodic Fibonacci structure (right) formed by stacking layers according to Fibonacci sequence.¹²⁵ (i) 1D SAW PnC realized by rectangular-like periodic grooves on the (001) surface of crystalline silicon.¹²⁶ In (a)-(d), the experimental dispersion relations (full/open points) were measured by Brillouin light scattering and calculated by finite element method (FEM). Panel (a) shows a calculated transmission spectrum. (a)-(i) Reproduced with permissions from Zhu *et al.*, Phys. Rev. B **88**, 144307 (2013). Copyright 2013 American Physical Society; Beltramo *et al.*, Phys. Rev. Lett. **113**, 205503 (2014). Copyright 2014 American Physical Society; Alonso-Redondo *et al.*, Nat. Commun. **6**, 8309 (2015). Copyright 2015 Springer Nature; Graczykowski *et al.*, Nano Lett. **20**, 1883–1889 (2020). Copyright 2020 American Chemical Society; Graczykowski *et al.*, Phys. Rev. B **91**, 075414 (2015). Copyright 2015 American Physical Society; Dehghannasiri *et al.*, Phys. Rev. Appl. **10**, 064019 (2018). Copyright 2018 American Physical Society; Wagner *et al.*, Nano Lett. **16**, 5661–5668 (2016). Copyright 2016 American Chemical Society; Aliev *et al.*, J. Appl. Phys. **116**, 094903 (2014). Copyright 2014 AIP Publishing LLC; and Graczykowski *et al.*, Appl. Phys. Lett. **104**, 123108 (2014). Copyright 2014 AIP Publishing LLC.

the frequency stop bands were detuned, in addition to the lattice spacing, by the geometric parameters, i.e., size and shape of holes^{133,134} and pillars^{122,129,132,135,136} and by solid¹³⁷ or liquid inclusions.¹³³ Figure 4(e) illustrates two examples of PnCs, i.e., solid/air and solid/solid fabricated from 250 nm thick Si membrane.¹²² The solid-air PnC revealed BG for all types of Lamb waves and BG for symmetric modes, both about 13 GHz. The band diagrams of solid-solid PnC showed apparent hybridization of local resonances of pillars with propagating waves in the membrane, albeit HG was not detected. Overall, 2D PnCs offer a versatile platform for manipulation of confined (SAW and Lamb) acoustic signals in the GHz regime, which can be utilized in wireless communication devices. For example, PnC made from the periodically etched silica film on a quartz substrate was demonstrated as a 1.25 GHz one-port Love waves resonator.¹³¹ In addition, recent work reported piezoelectric and CMOS-compatible pillar-based PnCs [Fig. 4(f)]. The experimentally measured transmission spectra revealed a 150 MHz wide SAW bandgap with the central frequency at about 1.65 GHz.¹²³

Both for top-down and bottom-up approaches structural imperfection is an unavoidable issue. Nevertheless, the deviation from the ideal translational order of the lattice can lead to new phononic features. In particular, the disorder can destroy the coherent effects as it was experimentally proved for the example of holey Si membrane illustrated in Fig. 4(g).¹²⁴ Also, theoretical studies revealed that the disorder could result in bandgap broadening and acoustic Anderson localization in PnCs.^{138,139} Undoubtedly, both works deserve experimental verification in the near future.

One-dimensional (1D) hypersonic PnCs are relatively less complex structures than previously discussed 2D and 3D PnCs. However, they can offer distinct phononic behavior for BAWs, SAWs, or Lamb waves propagating parallel or perpendicular to the periodicity. In practice, 1D bulk PnCs are superlattices (SLs), i.e., stacks of periodically alternating layers of different elastic impedances.^{143–147} 1D PnCs are straightforward systems, which can host both phononic and photonic bandgaps. The first direct measurement of the hypersonic phononic bandgap in SiO₂/PMMA SLs was reported by Gomopoulos *et al.*¹⁴⁸ The Brillouin light scattering (BLS) results revealed that the BG in such PnCs could be altered through the porosity of SiO₂ layers. The lattice imperfections, defects, or aperiodicity were investigated experimentally in terms of new phononic effects. The defects were investigated by probing the acoustic transmission¹⁴⁹ and dispersion relation (BLS).¹⁴⁷ Going further, the aperiodic (quasiperiodic) 1D Fibonacci SLs [Fig. 4(h)] were studied employing acoustic transmission¹²⁵ and femtosecond pump-probe spectroscopies.¹⁴⁶ In this case, the aperiodic structures were found as better acoustic filters than their ordered counterparts. In the case of the lattice disorder, acoustic Anderson localization was predicted theoretically for GaAs/AlAs SLs.¹⁵⁰ The propagation of SAWs in surfaces periodically corrugated in one dimension was theoretically studied already in the 70s. The recent experimental realizations of hypersonic 1D SAW PnCs were examined by BLS and pump-probe experiments.^{126,129} Figure 4(i) displays SEM image of PnCs made out of rectangular-like periodic grooves made on the (001) surface of crystalline silicon.¹²⁶ This system revealed hypersound filtering due to BG in the

direction perpendicular to the grooves, while along the grooves, it worked as a waveguide for Lamb waves confined in the stripes. Recently, 1D gourd-shape PnC tethers showed reduced anchor losses and improved quality factor for Lamb wave resonators in the GHz range. This single-chip system can be potentially explored for applications for wireless communication devices.¹⁵¹

B. Metamaterials made of low-dimensional nanostructures

The PnCs mentioned so far have their bandgaps centered around 1–20 GHz. To achieve higher frequencies (~100 GHz to 1 THz) the PnCs need to have smaller feature sizes, i.e., in the order of tens to few nanometers. This downscaling implies a major challenge for standard nanofabrication techniques. Potentially, smaller PnCs can be assembled by low-dimensional materials like nanoclusters or quantum dots (0D), nanotubes or nanorods (1D), and graphene-like materials (2D).

0D building blocks for nanodevices (e.g., quantum dots of chalcogenides and perovskites) have been widely studied due to their potential applications in optoelectronic devices, light-emitting diodes, photodetectors, and solar cells.^{152,153} Notably, 0D structures of chalcogenides like CdSe, CdS, and PbS can self-assemble and form CCs.^{140,154–157} The available literature is comparably extensive for colloids based on perovskites such as mixed-halide nanocrystals,¹⁵⁸ or organometal halide perovskites.¹⁵⁹ More information on semiconducting colloids can be found in previous reviews.^{152,153,160} Such systems have already been considered for the construction of photonic crystals.^{159,161} In comparison with photonics, the application of 0D semiconductors in phononic devices is limited. However, acoustic phonons and various other structural motions affect the electronic states and optical properties of chalcogenide and perovskite colloids and crystals.^{162–166} Regarding extrinsic interactions, scattering of SAWs on supported quantum dots can modify their energy levels.¹⁶⁷ This interaction enables various interesting applications at the interface of phononics and optoelectronics, which involve control of semiconducting quantum dots with SAW devices.¹⁶⁸ Based on all the above, CCs made of 0D semiconducting nanostructures represent a new type of phononic metamaterial that deserves additional experimental investigations—see Fig. 5(a) and the work of Yazdani *et al.*¹⁴⁰

While the formation of CCs relies on the spontaneous behavior of 0D nanostructures (self-assembly), the synthesis of metamaterials out of 2D nanostructures can be more controlled. For instance, 2D PnCs can be fabricated by patterning transition metal di-chalcogenides (TMDCs)—see Fig. 5(b) and the work of Munkhbata *et al.*¹⁴¹ These graphene-like materials have attracted considerable attention over the last decade. Thus, their mechanical, electronic, thermal, and optical properties are relatively well known. TMDCs are also termed layered materials and van der Waals (vdW) materials. This means that their atoms are arranged in 2D layers held together by weak vdW bonds. Hence, various TMDCs, like MoS₂, MoSe₂ and WS₂, can be prepared in the form of ultra-thin membranes.^{169–173} The thickness of TMDCs can be as small as one layer using liquid¹⁷⁴ or mechanical¹⁷⁵ exfoliation from the bulk. In order to employ these materials as 2D PnCs, it is necessary to introduce periodic patterns. This can be achieved in various

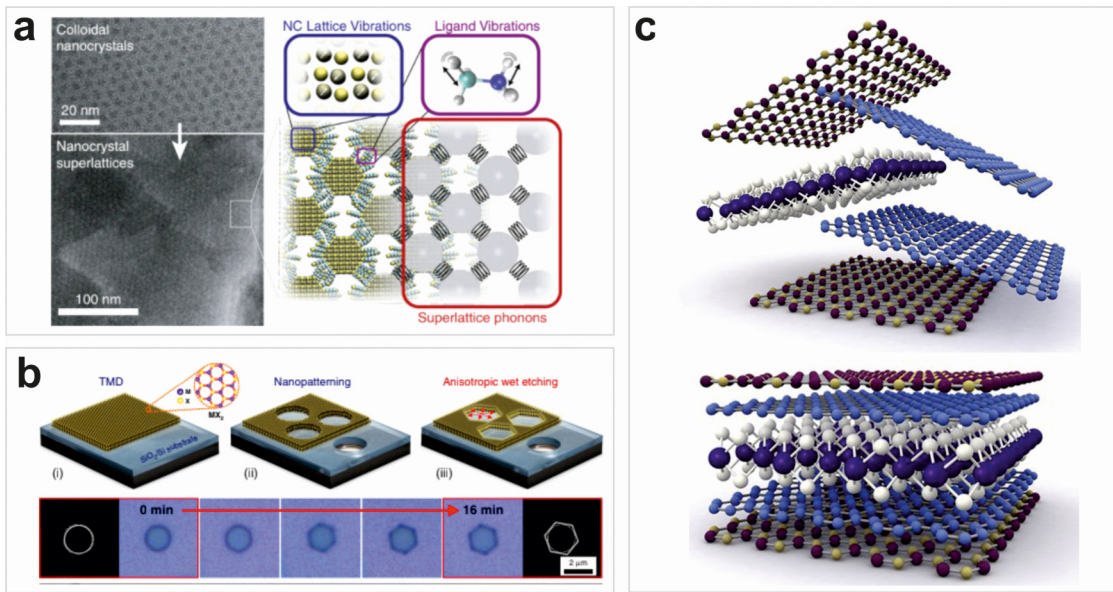


FIG. 5. Novel materials for nanophononics. Colloidal crystals made of ultrasmall semiconducting nanocrystals linked with polymeric ligands.¹⁴⁰ (b) Nanopatterning and wet etching of supported TMDCs thin films.¹⁴¹ (c) Illustration of 1D heterostructures made of vdW layered materials.¹⁴² (a)–(c) Reproduced with permissions from Yazdani *et al.*, Nat. Commun. **10**, 1 (2019). Copyright 2019 Springer Nature; Munkhbat *et al.*, Nat. Commun. **11**, 4604 (2020). Copyright 2020 Springer Nature; and Novoselov *et al.*, Science **353**, aac9439 (2016). Copyright 2016 AAAS Publishing.

ways. For instance, Yun *et al.* created nanopatterns on supported MoS₂ by block copolymer lithography.¹⁷⁶ Munkhbat *et al.*¹⁴¹ created TMDC metamaterials with a three-step process: (i) transfer of mechanically exfoliated TMDCs on a desired substrate, (ii) use of nanopatterning techniques like EBL, RIE, or focused ion beam (FIB) and (iii) anisotropic wet etching [Fig. 5(b)]. This approach offers perforated TMDCs (like WS₂, MoS₂, and MoSe₂) with nearly atomically sharp zigzag edges.¹⁴¹ Moreover, FIB can be used to introduce single-atom defects/holes in free-standing monolayer TMDCs.¹⁷⁷ Kozubek *et al.*¹⁷⁸ used highly charged ions to drill well-defined pores in free-standing MoS₂ with sizes of several nanometers. Irradiation with He⁺ has also been used to perforate free-standing TMDCs (MoS₂).¹⁷⁹ Additionally, linear patterning of TMDCs¹⁷⁶ can be used to prepare metamaterials with grooves. Zhang *et al.* moved a step further and demonstrated atomically thin photonic crystals made of square arrays of holes on free-standing WS₂.¹⁷³ Additional flexibility in the design of TMDC metamaterials can be achieved with nanopatterning of vdW heterostructures as the ones illustrated in Fig. 5(c).¹⁴² In this case, the system will act as a 1D superlattice normal to the layers and as a 2D metamaterial parallel to them.

The use of low-dimensional nanomaterials to construct novel PnCs will introduce new challenges for experimental and theoretical studies in phononics. Widely adopted experimental techniques like BLS, pump-probe measurements, Raman, x ray, and neutron scattering will have to deal with the poor signal-to-noise ratio due to the small dimensions of the samples. Spectroscopic techniques based on inelastic light scattering (for instance, spontaneous BLS)

will be limited by the opaqueness of the samples and the high frequencies (small thermal occupations) of acoustic phonons. Moreover, the confined acoustic phonons are expected to be affected by various microscopic couplings that need to be measured. For instance, the use of metallic, semiconducting, or magnetic nanomaterials will enable couplings of acoustic phonons with plasmons, electron-hole pairs, and magnons. We believe that many of these challenges can be addressed with pumped-BLS, a recently developed hybrid technique that combines ultrafast photoexcitation of confined acoustic phonons with BLS detection in frequency-domain.¹⁸⁰ This technique offers 100-fold amplification of BLS signal from semiconducting nanomembranes and reveals interactions of acoustic phonons with charge carriers—see Vasileiadis *et al.* for further details.¹⁸⁰

IV. OPTOMECHANICAL CRYSTALS

Optomechanical (OM) coupling is based on the commensurated wavelength of GHz phonons and electromagnetic radiation for telecommunications. The most important platforms for microelectronics and photonics, such as silicon and silicon nitride, allowed the demonstration of OM coupling in micrometer size cavities.¹⁸¹ OM coupling exploits co-localization of phonons and photons to maximize the energetic exchange between them. This paves the way for manipulating the phonon population in various ways. For instance, using OM coupling it is possible to decrease the average population below 1 in selected modes (ground state cooling¹⁸²—red detuned light excitation) or to generate amplified

coherent phonon emission¹⁸³ (blue detuned light excitation and phonon lasing). In the same kind of cavities, other schemes exploit optical free carrier generation and thermal dynamics to generate self-sustained amplified phonons at lower frequencies.¹⁸⁴

Optomechanics is a huge research field with a plethora of promising applications in telecommunications and sensors (e.g., memories¹⁸⁵ and accelerometers¹⁸⁶). It has a long term vision in quantum computation exploiting coherent phonon manipulation¹⁸⁷ and in topological phonon propagation with OM as driving effect.¹⁸⁸ In this direction, plenty of efforts have been devoted to increasing phonon lifetime by shielding the structures from the sources of dephasing. This can be achieved either by surrounding the OM cavities with a structure that has a phonon bandgap or with appropriately selected unit cells that provide their own bandgap in 1D¹⁸⁹ [Fig. 6(a)] and 2D¹⁹⁰.

In particular, self-driven OM oscillators are ideal building blocks for exploring the collective dynamics of networks of coupled oscillators.^{191,192} The observation, control, and exploitation of collective phenomena such as synchronization can find various applications. Some examples are neuromorphic computational platforms, on-chip robust time keepers, and sensors of mass, gas, or force with extremely low phase noise. Experimental observation of synchronization phenomena in pairs of coupled OM oscillators^{193,194} has been already reported and scaling up the number of coupled oscillators will not increase substantially the technological requirements.

We center now our attention to the capability of OM systems for ultrasensitive sensing of mechanical wave propagation using light (transduction), which is essential to build circuit functionalities using phonons. This can be done by placing an optomechanical transfer gate, in the form of an integrated optomechanical cavity¹⁹⁵ or by visualizing the movement of an antenna-like mechanical resonator coupled to propagating phonon modes.¹⁹⁶ In the latter case, the phonon modes are visualized by analyzing the modulation of a

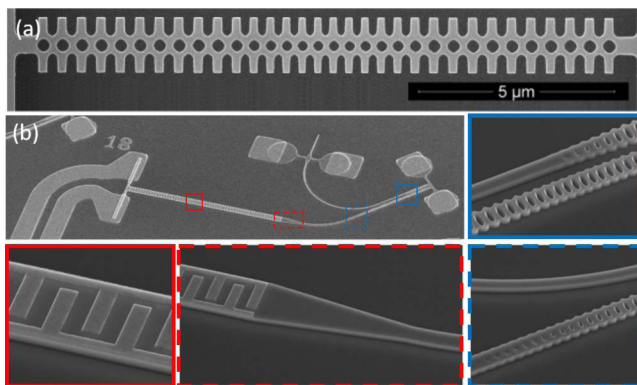


FIG. 6. Optomechanical crystals. (a) 1D OM crystal with full Phononic bandgap. Reproduced with permission from Navarro-Urrios *et al.*, Sci. Rep. **5**, 1–7 (2015). Copyright 2015 Springer Nature. (b) Scanning electron micrographs (SEM) of one piezo-optomechanical transducer. Zoomed-in SEMs show the conversion region between microwave and mechanics (red) and between mechanics and optics (blue) from Ref. 197. Copyright 2020 Springer Nature.

reflected beam. This capability is particularly technologically relevant as it is currently being extended to bridge the transfer of information between microwaves, electrically and optically modulated signals in an energy efficient way. Hybrid systems, including piezoelectric and optomechanical systems, report the highest yields in the GHz regime at modest power dissipation. Using the standard LiNbO₃ platform¹⁹⁷ [Fig. 6(b)], we can cover a crucial demand of our information society to build efficient transceivers for the huge data centers that operate nowadays. In such systems, a microwave signal incident on an Interdigital Transducer (IDT) is converted to a propagating phonon that is guided toward an OM cavity. In the OM cavity, the phonon modulates an optical signal. This process is bidirectional: a modulated optical signal injected in the circuit can excite mechanical motion in the OM cavity, which is then guided toward the IDT to generate a microwave signal.

To make these systems more compact, various works explored other mechanisms of efficient GHz phonon generation that can replace IDTs. The first proof-of-concept experiment,¹⁸³ where GHz phonons are generated in an OM cavity routed by phononic waveguides and transduced back to the RF signal by another OM cavity, have been followed by studies to increase phonon lifetime. Efforts to minimize phonon waveguide losses have exploited phononic bandgap acoustic shielding,¹⁹⁸ engineering of elastic strain,¹⁹⁹ and topologically protected edge states.²⁰⁰

V. THERMAL TRANSPORT

Phonons are the primary heat carriers in solid dielectrics and semiconductors. According to Bose-Einstein statistics, at room temperature (RT), phonons of frequencies up to several THz are excited.^{3,201} Notably, this broad-spectrum contributes to the transport of the vibrational energy and can be effectively tailored by the spatial nanoconfinement.^{202–205} The recent remarkable progress in the field of the nanoscale thermal transport has proven the breakdown of Fourier's law in spatially confined systems. Some examples of phenomena that go beyond the classical description of heat transport are strong suppression of the phononic thermal conductivity, wave-like propagation of heat, observation of the second sound in solids at moderate temperatures, thermal cloaking, and focusing and rectification.^{4,21} Nowadays, it is clear that confinement of thermal phonons in the micro- and nanoscale offers fascinating features and challenges in their transfer to the mainstream technology applications. In the following, we first distinguish between coherent and incoherent effects in thermal transport, and then we discuss the potential of thermal phonon management for applications like thermoelectrics and controlled heat transport in devices.

A. Coherent and incoherent effects

To explain the basic concepts of nanoscale thermal engineering, we recall the kinetic theory, which defines the phononic thermal conductivity as $\kappa \propto C v_g \Lambda$.²⁰³ Here, C is the heat capacity, v_g denotes the average group velocity, and Λ stands for the mean free path (MFP) of phonons. The latter parameter is an average distance traveled by a phonon between two scattering events, which can occur on impurities, imperfections, phonons (umklapp), electrons, and boundaries.^{3,21,203} Notably, this much-simplified

description allows for a good estimation of thermal conductivity for various materials. Furthermore, it points to phonon MFP and group velocity as being essential to alter the thermal conductivity. The research from the last decade has revealed that both of these quantities can be modified using PnCs with sub-micrometer feature size.^{4,21,206–222} Indeed, shortening of the phonon MFP can result from imperfections between periodic motives and the matrix constituting PnCs. In this case, the interface roughness is comparable with the wavelength of thermal phonons. Thus, thermal phonons behave like particles that are diffusively scattered on the interfaces. As the phase is not preserved, this phenomenon is referred to as the incoherent effect.^{8,21,223}

The second-order periodicity of PnCs alters the phonon dispersion relation, which implies reduced v_g , altered DOS, and under certain conditions, phononic bandgaps.^{8–10,122} This approach utilizes the wave nature of phonons, and it requires both specular reflections from interfaces and MFPs of phonons (more rigorously phonon coherence length) that are at least a few times longer than the PnC periodicity. This phenomenon is referred to as the coherent effect in the literature, while PnCs are termed thermocrystals.^{21,212} Unambiguous experimental evidence for the coherent heat conduction, thermal phonon localization, and crossover from coherent and incoherent regimes was demonstrated for 1D PnCs (superlattices). Notably, such phenomena to be observed at room temperature require structures of dense and atomically smooth interfaces.^{215–217}

The dual, wave-particle nature of thermal phonons in 2D PnCs is a topic of ongoing widespread debate. Numerous works have reported reducing phononic heat conduction in membranes of periodic porosity with respect to the pristine membrane. The controversial issue that has arisen is the contribution of coherent effects near room temperature in PnCs with lattice parameter greater than 100 nm.^{124,206,208,211,221,224,227,228} In this case, the relevant PnCs were made using electron beam lithography (EBL) and reactive ion etching (RIE) or focused ion beam (FIB) milling (see examples in Fig. 7). Both approaches allow the fabrication of holes with roughness of few nanometers, in the best scenario, and amorphization.^{128,206,211} To date, a real demonstration of the coherent effects was only possible at few Kelvin and sub-Kelvin temperatures for Si and Si_3N_4 PnCs, respectively.^{211,212} In these conditions, heat is carried via long MFP, GHz phonons of about micrometer wavelengths that are much larger than the surface roughness. On the other hand, in bulk Si at room temperature, MFPs span a broad range, and those longer than one μm contribute to $\sim 50\%$ of the total thermal conductivity at room temperature. In general, this allows thermal phonons to travel over several lattice periods of PnCs and interfere, and thereby manifest wave-like nature. Accordingly, some of the prior works explained the suppression of κ as a combination of incoherent and non-negligible, coherent effects.²²¹ Recent works, based on indirect and direct methods, have not confirmed those results. Namely, the disordered and aperiodic PnCs show the same thermal conductivity as their ordered counterparts [Fig. 7(b)].²⁰⁶ More directly, results obtained using BLS¹²² and Asynchronous Optical Sampling¹²⁴ (ASOPS) have confirmed modification of the phonon dispersion up to tens of GHz, what is relevant at very low temperatures but negligible at RT. Furthermore, two-phonon Raman spectra [Fig. 7(c)] that reflect phonon DOS

proved no difference between spectra of PnCs and pristine membrane in the THz.²⁰⁸ Even though the concept of the room temperature thermocrystal is doable, it can only be implemented in PnCs of the few-nanometer period and atomically smooth interfaces.²¹

B. Perspectives and applications

Further development of PnCs dedicated to the management of thermal phonons can result from application-oriented directions such as thermal energy harvesting, extreme temperatures and gradients, effective heat dissipation, geometry engineering toward ray-like heat transfer, the synergistic combination of conduction with convection or radiation, and thermal rectification, new materials as platforms for PnCs, and materials hosting other elementary excitations being, in addition to phonons, heat carriers.

The reduced thermal conductivity in 2D porous PnCs holds great potential for applications in thermal energy harvesting, sensing, and heat flow management.²²⁹ In particular, crystalline porous Si membranes can be used to realize Slack's "phonon glass-electron crystal," i.e., hypothetical material of maximized thermoelectric (TE) figure of merit ZT .²³⁰ Hence, the perforation leading to κ as low as the amorphous limit has to maintain the electronic properties. The latter can be further engineered by doping toward an optimized electronic power factor. Yet, recent works have reported TE generators made of porous Si membranes with $ZT \ll 1$ around RT, which is significantly less than what is offered by conventional materials.^{210,213,214,229} However, Si PnCs are CMOS-compatible and therefore can be easily implemented in mainstream technology. For instance, the upcoming market of the Internet of Things can benefit from cheap and robust self-powered units or sensors based on such structures.

Furthermore, silicon and silicon on insulator (SOI) technologies are the most mature for producing micro- and nanoscale devices dedicated to high-temperature applications.²³¹ The high temperature is a considerable value market for thermal sensing and energy harvesting in the automotive, aerospace industry, space exploration, metallurgy, and conventional energy production.²³² Besides a few recent works,^{208,219} thermal properties of PnCs at temperatures exceeding 500 K remain primarily unexplored area due to experimental challenges. Thus, novel tools based on, most likely, contactless approaches are needed [Fig. 7(h)].

As follows from theoretical works, local resonances can be an alternative approach for thermal phonon blocking in 2D PnCs. In this concept, PnCs consist of a 2D array of pillars deposited on the membrane. In this structure, the hybridization between localized modes in pillars and propagating modes in the membrane results in sub- and super-wavelength bandgaps that are immune to the PnC lattice's imperfections.^{233,234} Besides that, typical phononic effects can appear due to the periodic arrangement of pillars. Consequently, phonon group velocity, DOS, and hence thermal conductivity can be tuned (in addition to lattice spacing) by the characteristic sizes and mass of the pillar. The modification of the dispersion in these structures was confirmed experimentally for GHz phonons employing BLS.²³⁵ However, the importance of coherent effects on the thermal conductivity has been recently questioned based on the experimental results obtained in the 4–300 K range.^{225,236}

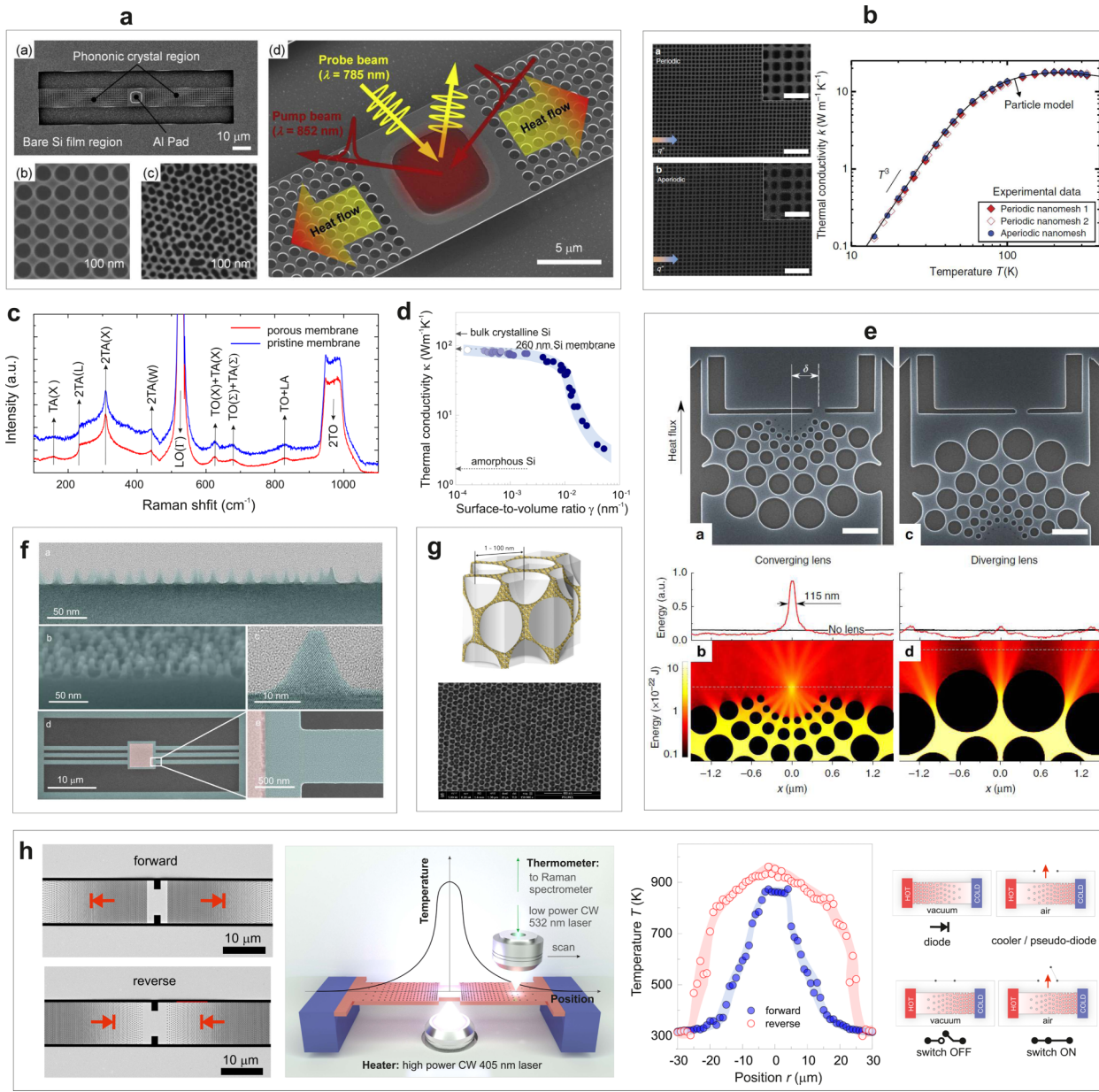


FIG. 7. (a) SEM images of the Si PnCs fabricated in a suspended architecture for thermal reflectance measurement.²¹⁸ (b) SEM image of a (left panel) periodic Si nanomesh with a period of 100 nm and (middle panel) an aperiodic Si nanomesh with the pitch varied from 80 to 120 nm. Scale bars are 200 nm (inset) and 600 nm (main). (right panel) Measured thermal conductivities of periodic and aperiodic nanomeshes as a function of temperature indicate the negligible role of the coherent effects.²⁰⁶ (c) One- and two-phonon Raman spectra of pristine 250 nm membrane without and with pores obtained at room temperature. The critical points of the first Brillouin zone are identical for both samples.²⁰⁸ (d) Thermal conductivity of porous membranes at 300 K as a function of the surface-to-volume ratio.²¹⁹ (e) SEM images of (left upper panel) converging and (right upper) diverging thermal lens samples with slits for heat dissipation. The scale bar is 1 m. Monte Carlo simulations results of (bottom left) the formation of a hot spot in the focal point and (bottom right) dispersion of heat in the diverging lens.²²⁴ (f) TEM and SEM images of 20 nm-high nanopillars fabricated on 50 nm-thick silicon membranes.²²⁵ (g) A scheme and SEM image of a metalattice made of a closely spaced distribution of spherical voids in crystalline silicon.²²⁶ (h) From left to right: SEM images of the thermal rectifiers in the forward and reverse configurations, schematic of the two-laser Raman thermometry experiment, temperature profiles of the test devices in the forward (solid purple circles) and reverse (red-outlined circles) configurations, schematics of possible devices based on the thermal rectifier.²¹⁹ (a)–(h) Reproduced with permissions from Lee *et al.*, Nat. Commun. **8**, 14054 (2017). Copyright 2017 Springer Nature; Takahashi *et al.*, Nano Energy **71**, 104581 (2020). Copyright 2020 Elsevier Ltd.; Anufriev *et al.*, Nat. Commun. **8**, 15505 (2017). Copyright 2017 Springer Nature; Huang *et al.*, ACS Appl. Mater. Interfaces **12**, 25478–25483 (2020). Copyright 2020 Elsevier Ltd.; and Chen *et al.*, ACS Nano **14**, 4235–4243 (2020). Copyright 2020 American Chemical Society.

Recently, Anufriev and Nomura have proposed a concept of ray phononics utilizing ballistic heat transport in porous membranes.²²⁴ Such materials are envisioned for ray-like heat flow management in nanostructures regardless of their surface imperfections and foremost possible at room temperature. The proof-of-concept experiments have proved features like thermal phonon guiding, emission, and focusing [Fig. 7(e)].

Needless to say that wealth of new features resulting from the phonon confinement go hand in hand with technological challenges. Indeed, the progress of miniaturization and electronic devices' performance in the last two decades has encountered a bottleneck related to the efficient removal of the produced heat. Thus, both size-reduced thermal conductivity and volume can lead to overheating and eventually damage of nanoscale components. Porous membranes can be an effective and low-cost solution to this problem, which utilizes passive cooling units via air convection. Simultaneously, the vast majority of previous thermal studies of porous membranes were performed in vacuum conditions. However, convection in porous membranes deserves more attention regarding the real conditions for their operation and possible application in passive cooling. As follows from recent experiments, the heat dissipation via combined convection and conduction can be optimized via the structure surface-to-volume [Fig. 7(d)] ratio.^{208,219}

The enhancement of the heat dissipation in nanostructured membranes (depending on the material) can be seen in less obvious elementary excitations such as surface phonon-polaritons (SPhPs), magnons, or plasmons. Wu *et al.* have demonstrated that the thermal conductivity of sub-50 nm thick Si₃N₄ membranes doubles as the temperature increases from 300 to 800 K due to SPhPs.²³⁷ In this Perspective, new architectures of PnCs can primarily benefit from a synergistic combination of dielectric or semiconducting membranes with metallic and magnetic layers or nanostructured motives. In particular, the emerging fields of spin caloritronics^{238,239} and the intersection between plasmonics and phononics²⁴⁰ are attractive directions for further developing the nanoscale thermal transport in periodic structures. Another and quite natural step forward can be the fabrication of macroscale 3D PnCs for thermal flow management using self-assembled colloidal crystals,^{241,242} metatlattices,²²⁶ or atomic quality hybrid (organic-inorganic) Bragg stacks.²⁴ Notably, the aim of the latter materials is, contrary to the majority of PnCs, to enhance the thermal conductivity to remove process heat in organic electronics preserving transparency and flexibility.

One of phononics' main ambitions is to use heat as the information carrier and develop thermal analogs of diodes, transistors, and electronics switches.^{4,243–245} The fundamental requirements for a thermal diode (or rectifier) can be satisfied by porous membranes. Namely, they offer temperature dependence of the thermal conductivity (non-linearity) and space dependence (spatial asymmetry) of the thermal conductivity. Practical realization of thermal rectification was reported for perforated graphene (26% efficiency at RT)²⁴⁶ and recently for Si membrane. The latter structure (14% efficiency) is dedicated to operation at high temperatures up to 1000 K and can also be utilized as a thermal switch or optimized convective cooler [Fig. 7(h)].²¹⁹

Overall, the future of PnCs requires new platforms that can host phononic effects and introduce new physical and chemical

features. From this Perspective, an excellent opportunity is the wealth of van der Waals materials, and their heterostructures offer unique, highly anisotropic, and size-dependent electronic, optical, thermal, and mechanical properties.^{142,247–249} Nevertheless, this requires a significant advancement in the fabrication of robust large area samples and experimental tools development.

VI. TOPOLOGICAL PHONONICS

A. From symmetry to topology

Up to this point, we discussed phononic metamaterials whose properties depend solely on the crystal symmetry and are strongly affected by defects and disorder. The relevant transport phenomena are characterized by losses, left-right symmetry (parity, *P*), and time-reversal symmetry (*T*) and/or principles of thermodynamics. This section presents a novel type of metamaterials, termed topological phononics, which offers robustness to disorder, one-way propagation of phonons (broken *P* or *T* symmetry) and transport without losses. In most cases, the different phases of condensed matter are adequately characterized by distinct symmetries, and a symmetry-related order parameter describes the passage from one phase to another. However, it is possible to observe phases of matter that do not depend on the sample's size, shape, composition, and impurities. The unique identification of such phases requires some topologically invariant property, meaning a property that remains constant under continuous transformations.

Topology has first entered the realm of experimental, condensed matter physics in 1980 with the discovery of the Quantum Hall Effect (QHE) by Von Klitzing *et al.*²⁵⁰ The QHE is the quantized Hall conductance of a two-dimensional (2D) electron gas in a strong magnetic field and at low temperature. Subsequent studies revealed several more types of topological phenomena for electrons and spins in crystals. For instance, in the Quantum Spin Hall Effect²⁵¹ (QSHE) the spin Hall conductance of 2D crystals is quantized due to spin-orbit coupling without a magnetic field. Another relevant electronic degree of freedom is the valley, i.e., the bands extreme that the electrons occupy, which gives rise to the Quantum Valley Hall Effect^{252,253} (QVHE). The observation of topological phenomena in three-dimensional (3D) crystals gave rise to the so-called topological insulators.^{254,255} In these materials, the topology of the bulk states is distinct from that of the surrounding vacuum, leading to the creation of unique, conductive surface states. Dirac semimetals are insulating in the 3D bulk and have 2D surface states with Dirac cone dispersion.²⁵⁵ Weyl semimetals have topologically protected Dirac cones in the 3D bulk, and surface states with unique, arc-shaped dispersion.^{256–259} Additionally, Floquet topological insulators have conductive surface states due to external, periodic, temporal perturbations.^{260,261} From the perspective of basic science, topological condensed matter systems can be used to perform tabletop experimental studies of exotic particles that remain unobserved in nature, like magnetic monopoles,^{262–264} as well as Dirac and Weyl fermions.²⁵⁵

The first experimental realization of topological phenomena for classical waves and metamaterials occurred in 2009 by Wang *et al.*²⁶⁵ who demonstrated a topological photonic metamaterial operating in GHz frequencies (microwave radiation). The readers can find more information about topological photonics in the

review articles of Lu *et al.*²⁶⁶ and Ozawa *et al.*²⁶⁷ The first topological acoustic metamaterial was realized by Fleury *et al.*²⁶⁸ in 2014. This acoustic crystal consisted of ring resonators, where left-handed and right-handed modes were initially degenerate. The degeneracy was then removed with a biasing airflow, leading to one-way transport of sound. Topological phononics have been discussed in a number of previous review articles.^{269–271} Here, after a short introduction, we emphasize the novel topics of 1D topological phononics, higher-order topological insulators, and programmable topological phononics. Next, we discuss how the various macroscopic designs can be re-adapted for topological nanophononics in the gigahertz (GHz) frequency range. We conclude this section with a proposal on studying low-dimensional, topological nanophononics in the GHz range, using a recently developed combination of Brillouin spectroscopy and ultrafast photoexcitation.

B. Topology for condensed matter physics

In the band structure theory of insulators, topology is used to examine if one insulator can be smoothly transformed into another. If this is not the case then a topological phase transition must occur at their interface leading to the creation of spatially confined conductive states. As an example to describe Chern insulators, the starting point for defining the topologically invariant property is the Berry phase^{272,273} (γ), which is used to describe the change of a quantum state with respect to some variable ($X(t)$) of the system's Hamiltonian that changes slowly with time (adiabatically). In condensed matter physics, the X is the wavenumber k (of electrons, phonons, or other quasiparticles), and the adiabatic change is a motion in reciprocal space. If this motion follows a closed path, and for a 2D crystal, the Berry phase is given by

$$\gamma = \oint \mathbf{A}(\mathbf{k}) \cdot d\mathbf{k}. \quad (1)$$

Here, $A = i\langle \phi_{nk} | \nabla_k | \phi_{nk} \rangle$ and it is called the Berry connection or the Berry potential^{272–274} (in analogy to the vector potential of electrodynamics). The function ϕ_{nk} is taken from the Bloch theorem: $\Psi_{nk}(\mathbf{r}) = e^{i\mathbf{k}\cdot\mathbf{r}} \phi_{nk}(\mathbf{r})$. Next, the Berry phase can be re-written as $\gamma = 2\pi C$, where C is the Chern number,²⁷³ which is the topologically invariant property of the Chern insulators according to the Thouless–Kohmoto–Nightingale–den Nijs (TKNN) theory.²⁷⁵ Using the Stokes theorem and relationship 1, the Chern number is given by

$$C = \frac{1}{2\pi} \iint_{BZ} \nabla \times \mathbf{A} d^2k. \quad (2)$$

The integration is over the entire Brillouin zone (BZ). Due to periodic boundary conditions, the integration area is also called the Brillouin torus.²⁷⁴ The vector field $\nabla \times \mathbf{A}$ is called the Berry curvature.^{272–274} The integral of relationship 2 is the flux of the Berry curvature field through the Brillouin torus. To achieve interesting topological properties (e.g., topological surface states, one-way transport and robustness to disorder), the Brillouin torus must contain a source of the Berry curvature field giving a non-zero Chern number. For plane waves or vacuum, the ϕ_{nk} is

constant and $C = 0$. Thus, if the bulk has insulating states with $C \neq 0$, a topological phase transition occurs at the surface with the emergence of gapless surface states. Similarly, confined gapless states appear at the interface between topologically distinct insulators (different Chern numbers). The latter topological phase transitions can be viewed as a band inversion—for instance, see the schematic illustration from Zhang *et al.*²⁷⁶ in Fig. 8(a).

C. Macroscopic topological phononics in various dimensions

In one-dimensional (1D) phononic crystals, topological edge states are localized oscillations without transport. Topological properties in 1D can arise due to some spatial modulation, e.g., of losses²⁷⁷ [Fig. 8(b)]. The topological acoustic crystal of Gao *et al.*²⁷⁷ [Fig. 8(c) left] has a bulk spectrum that is depleted at ~ 2150 Hz [Fig. 8(c) center], while the edges' spectrum has a maximum at the same frequency [Fig. 8(c) right]. Additionally, 1D phononic crystals have been shown to possess interfacial states²⁷⁸ (states between topologically distinct insulators) and Weyl particle physics.²⁷⁹

Since most of the relevant topological physics requires spin-dependent phenomena, several studies of acoustics explored acoustic pseudo-spin,^{284–288} acoustic QSHE,²⁸⁹ and acoustic analogs of spin-multipoles.²⁹⁰ Pseudo-spin-dependent transport was shown to be robust and to possess transmission without backscattering—see, for instance, Refs. 288 and 289. Pseudo-spin states can be formed in the presence of double Dirac cones. Double Dirac cones have been introduced in various ways, e.g., with zone-folding in a triangular lattice of rods,²⁹¹ or with 2D arrays of Helmholtz resonators,²⁹² or with local resonance states.²⁹³ Twofold Dirac point degeneracy appears for graphene-like phononic crystals²⁹⁴ and more complicated structures, like 2D kagome²⁹⁵ and Kekulé lattices.²⁹⁶ In the case of 2D square lattices, the Dirac cones can appear away from the high-symmetry points of the band-structure^{297,298}—a phenomenon described as accidental degeneracy. Moreover, 2D sonic crystals have been used to realize acoustic Floquet topological insulators.^{284,287} Notably, topological properties in 2D (or quasi-2D) systems can also arise from water surface waves.^{299–302}

Regarding 3D systems, He *et al.*³⁰³ showed that topological valley states can emerge at the interface of two crystals with opposite valley Chern numbers. Other studies using 3D metamaterials have demonstrated acoustic analogs of Weyl and Dirac semimetals,³⁰⁴ negative refraction,³⁰⁵ acoustic quadrupole³⁰⁶ and octupole^{307,308} topological insulators, and topological properties in granular metamaterials.³⁰⁹ Moreover, Peng *et al.*³¹⁰ have demonstrated 3D Floquet insulators, using a periodic, spatiotemporal modulation in a sonic crystal. Very recently, Fu *et al.*³¹¹ have studied sound vortices in 3D cylindrical waveguides and demonstrated diffraction of sound that depends on the value of the topological charge. In relevance with sound vortices, helical-acoustic metamaterials can be used for dispersion-free deceleration of sound³¹² and can potentially be useful for topological acoustic metamaterials.

A special type of topological materials termed higher-order topological insulators,^{280,295,313} support edge states that are two or more dimensions lower than the bulk states. For instance, in a third-order topological insulator, some of the states are confined

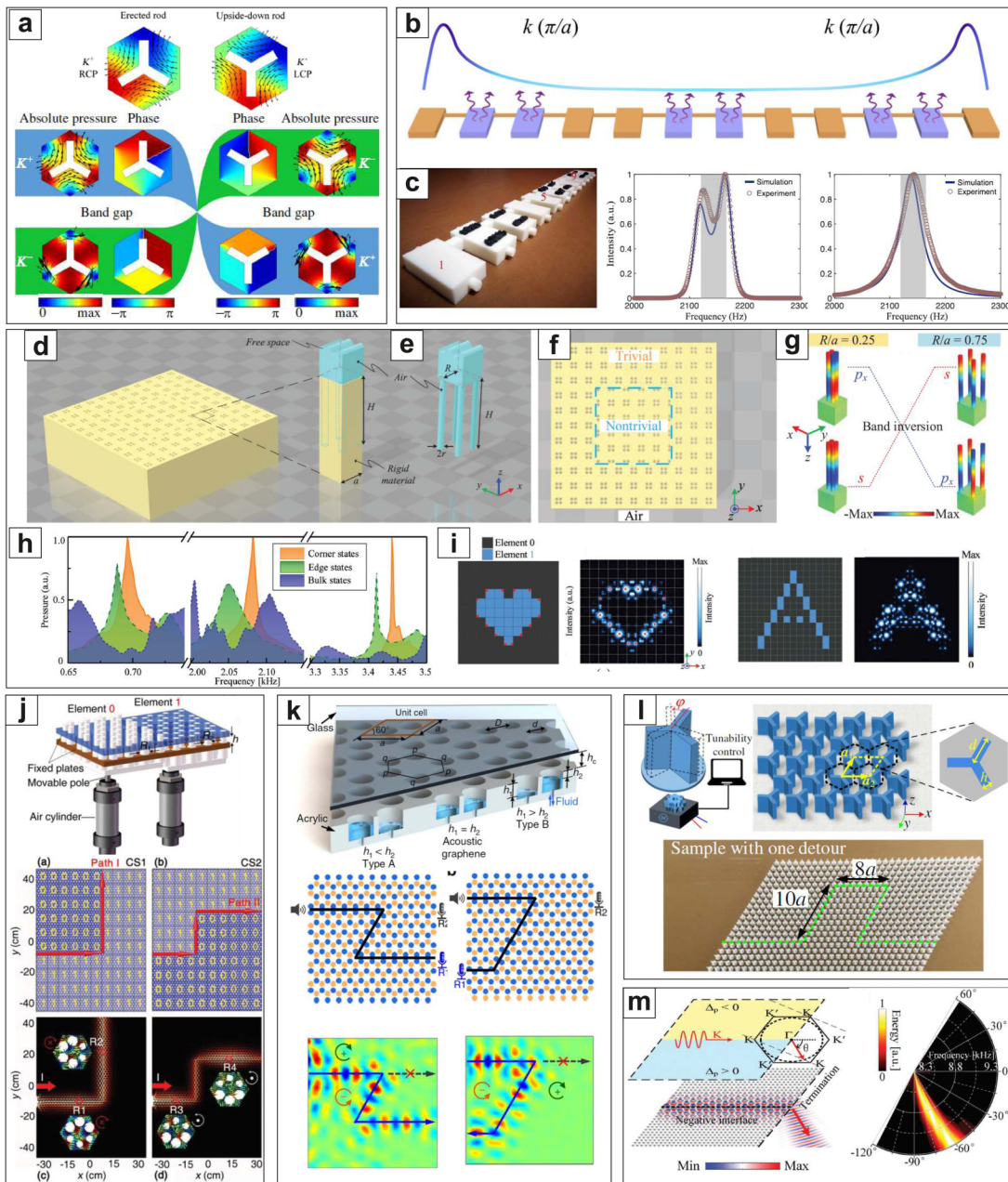


FIG. 8. Topological acoustics in 1D and 2D: (a) Rotatable three-legged-rods used to create spinning acoustic fields (up) and a topological phase transition of these acoustic pseudospin states (down) from Zhang et al.^[276] Copyrights obtained from 2018 American Physical Society. (b) Schematic of a 1D acoustic lattice with topological properties arising from spatial modulation of losses. Copyrights obtained from 2020 American Physical Society. (c) Image of the sample (left), acoustic resonances inside (center) and at the edges (right) of a structure studied by Gao et al.^[277] (d) Design of a second-order, 2D topological insulator.^[280] (e) its unit cell. (f) illustration of the boundaries between trivial and nontrivial topological regions. (g) diagram of the topological phase transition through band inversion. (h) VDOS for corner, edge and bulk states and (i) programmable patterns of acoustic fields. Tunable topological acoustics and applications: (j) Programmable 2D topological acoustic crystal controlled by pressurized air,^[281] (k) tunable 2D topological acoustic crystal using liquid infiltration,^[282] (l) acoustic delay line based on a tunable topological acoustic crystal,^[276] (m) directional emission of sound using topological acoustics.^[283] (a)–(m) Reproduced with permission from Zhang et al., Phys. Rev. Appl. 9, 034032 (2018). Copyright 2018 American Physical Society; Gao et al., Phys. Rev. B 101, 180303 (2020). Copyright 2020 American Physical Society; Zhang et al., Adv. Mater. 31, 1904682 (2019). Copyright 2019 John Wiley & Sons, Inc.; Xia et al., Adv. Mater. 32, 1805002 (2018). Copyright 2018 John Wiley & Sons, Inc.; Tian et al., Nat. Commun. 11, 762 (2020). Copyright 2020 Springer Nature; and Zhang et al., Adv. Mater. 30, 1803229 (2018). Copyright 2018 John Wiley & Sons, Inc.

on the corners (0D) of a 3D crystal.³¹³ Zhang *et al.*²⁸⁰ have demonstrated a second-order, 2D topological insulator, whose structure and properties are illustrated in Figs. 8(d)–8(i). Its unit cell [Fig. 8(e)] consists of four drilled holes; the yellow and the blue parts are the rigid materials and the air, respectively. This 2D crystal is split into two regions with trivial and nontrivial topological properties [Fig. 8(f)] by varying the ratio of the distance between holes R over the lattice constant a . Using finite element method (FEM), the authors have visualized the pressure distributions in the trivial and nontrivial regions and illustrated a band inversion from p- to s-like “conduction” states and from s- to p-like “valence” states [Fig. 8(g)]. The vibrational density of states [Fig. 8(h)], which was recorded using a loudspeaker and a microphone, shows 2D bulk states, 1D edge states, and 0D corner states, thus proving the second-order character of this topological acoustic crystal transport.

D. Programmable topological phononics and applications

Macroscopic metamaterials offer the possibility of real-time and on-demand structural changes. Thus, it is possible to control the topological properties in versatile, uncomplicated ways, and to construct smart devices for sound manipulation. For example, Zhang *et al.*²⁸⁰ generated programmable patterns of acoustic fields [Fig. 8(i)]. Xia *et al.*²⁸¹ have developed honeycomb-lattice sonic crystals that can be reconfigured with air cylinders [Fig. 8(j) top]. Using this design, the authors managed to control the path followed by the edge states between two topologically distinct phases [Fig. 8(j) bottom]. Tian *et al.*²⁸² have realized a tunable, sonic honeycomb lattice by infiltrating liquid in its holes [Fig. 8(k) top], which was again used to control the path of edge states [Fig. 8(k) bottom]. Zhang *et al.*²⁷⁶ constructed a hexagonal array of rotatable, three-legged elements [Fig. 8(l) top] that could be used as a phononic delay line [Fig. 8(l) bottom]. A prominent application of topological manipulation of sound is the construction of directional loudspeakers and microphones^{283,314} [Fig. 8(m)]. Regarding prospects, another exciting class of devices (which have not been experimentally realized at the moment for phononics) are one-way, topological, beam splitters.^{315–318}

Moreover, topological phononics support edge states with one-way transport^{284,289,319–321} and, thus, they can be used as phononic diodes^{219,322,323} or waveguides.³²⁴ It would then be interesting to use programmable topological phononics in order to construct switches and gates for phonons that mimic electronic circuits.^{90,91,325} Another interesting way for tuning the properties of topological phononic crystals is to take advantage of the physics of Floquet topological insulators, whose properties can be controlled by external fields, lasers, microwaves or other types of radiation.³²⁶ Finally, tunable topological acoustics can make use of soft, deformable materials.³²⁷

E. Topological gigahertz nanophononics

The topological phononic crystals mentioned so far have macroscopic dimensions, resulting in sound waves in the kHz to MHz frequency range. One of the most promising application of phononics is their use in wireless devices, where they mediate signal processing of microwaves. For such applications, the phononic

structures need to operate in the GHz range. The growing demand for signal processing at higher operational frequencies (5G wireless networks and beyond), and the vast progress of THz light technologies, will likely require phononic devices with higher operational frequencies. Higher operational frequencies can be achieved by spatial confinement of the phononic structures in the sub- μm to nm lengthscales (nanophononics).

Topological GHz nanophononics can be 1D systems like coupled nanocavity arrays.³²⁸ These 1D systems are GaAs/AlAs superlattices with band-inversion at the interface, while the probing technique can be in frequency- (Raman³²⁹) or time-domain (ASOPS³³⁰). Regarding 2D systems, several interesting, macroscopic crystals (e.g., hosting topological acoustic polaritons³³¹) can be scaled down to the sub-micrometer scale using lithographic techniques.^{8,128,205} Based on several theoretical proposals, experiments, and simulations, a good design for topological nanophononics is pillared phononic crystals.^{332–336}

Classical, macroscopic metamaterials can be precisely engineered in terms of their size, shape, and dimensionality. Thus, they can be used to evaluate the various designs and decide which of these can be transferred to the sub-micrometer lengthscale and GHz frequency range. For macroscopic 2D topological acoustics (see the work of Zhang *et al.*²⁸⁰), the experiments require sample-preparation by 3D printing, a loudspeaker to emit sonic waves and a microphone to detect the edge- and corner-states. For nanophononics, the 3D printing technology can be replaced by lithographic techniques.¹²⁸ Generation of coherent acoustic phonons can be carried out with ultrashort laser pulses—see, for instance, Arregui *et al.*³³⁰ The laser pulses generate coherent acoustic phonons through the thermoelastic effect and the displacement potential mechanism.³³⁷ The probing of topological phonons in 2D PnCs can be potentially performed by micro-BLS, which has the ability to map the vibrational density of states and the band structure,³³⁸ as well as the direction of phonons¹⁸⁰ (asymmetric Stokes/anti-Stokes intensities) with micrometer spatial resolution. Finally, a practical way of tuning the crystal properties might come from heterostructures of hard semiconductors and soft, polymeric structures. In such heterostructures, it will be possible to deform the soft matter part with an externally applied strain, and therefore to tune topological phase transitions at the interface.³²⁷ In this case, the additional usefulness of BLS is that it can measure directly and accurately the local strain, which causes flexural Lamb waves of zero momentum to have non-zero frequencies.^{339,340}

VII. SUMMARY

Research on PnCs is a relatively mature field that is more than 20 years old. The transition from research to the industry can be achieved for two types of PnCs: macroscopic sub-GHz PnCs for vibrational isolation and microscopic, hypersonic PnCs for MEMS and telecommunication. The design of PnCs can make use of various computational techniques like finite element methods,^{341,342} acoustic transfer matrix calculations,³⁴³ genetic algorithms,³⁴⁴ topological optimization,^{345,346} and machine-learning.^{63,347} These computational methods provide efficient but complex architectures that can now be realized with 3D printing technologies, sophisticated machining, molding and casting for

macroscopic PnCs, and bottom-up or top-down synthesis for microscopic PnCs—see the review article of Choi *et al.*³⁴⁸

Macroscopic PnCs with bandgaps at audible frequencies,^{314,344,346,349–356} and various acoustic metamaterials^{357–359} can be used for sound insulation of buildings, vehicles, and machinery. Moreover, macroscopic PnCs with non-trivial topological properties can be used to construct loudspeakers and microphones that control the direction^{283,314} and timing²⁷⁶ of sonic signals. Additionally, PnCs have promising applications for ultrasonic imaging in biomedical applications (Sec. II). Research on PnCs can even be useful for civil engineering and urban design. For instance, strategic planting of trees is the ultimate green method for protection against sound pollution³⁶⁰ and seismic waves.^{36–38} Protection from seismic waves can also be achieved with artificial, periodic structures called seismic metamaterials.³¹ Similar to seismic waves, PnCs and metamaterials that control water waves can be used for coastal engineering³⁶¹ and to amplify energy harvesting from ocean waves.³⁶²

Higher operational frequencies for phononic devices can be achieved through spatial confinement and nanostructuring. Thus, hypersonic PnCs have potential applications for signal processing applications at 5G frequencies and beyond. Apart from higher operational frequencies, PnCs for telecommunications need to maintain high-quality factors (minimize dissipation), which is one of the main advantages of phononic devices compared to electronic circuits.¹¹ The most critical missing component is a reliable source of coherent phonons that can operate at high frequencies ($\gg 10$ GHz). Likely, the development of coherent phonon sources at high frequencies can be facilitated by research on optomechanics (Sec. IV). So far, PnCs were mostly based on semi-transparent, insulating materials (e.g., SiO₂ and polymers like PS) and well-known semiconductors with 3D crystal structures like Si. The need for further miniaturization of phononic devices might be covered by novel, low-dimensional, semiconducting nanomaterials (Fig. 5). For instance, ultra-small 0D nanoclusters can self-assemble into colloidal crystals, and vdW layered materials can be used to construct ultrathin, crystalline metamaterials (Sec. III). However, the use of such novel nanomaterials will likely require a deeper understanding of microscopic interactions and dissipation processes for acoustic phonons. For instance, the use of metallic, semiconducting, and magnetic nanomaterials will require studies on the coupling of acoustic phonons with plasmons, excitons, and magnons, respectively. Additionally, metamaterials made of low-dimensional semiconductors can also be interesting in view of thermoelectrics (discussed in Sec. V). We expect that nanostructuring of 2D van der Waals materials¹⁴¹ or assembling carbon nanostructures with different dimensionalities³⁶³ will provide novel methods for thermal phonon management. The study and manipulation of thermal phonon transport can be useful for thermoelectrics or efficient cooling of electronic devices, but it is also fascinating from the perspective of basic research. Some examples are coherent effects in thermal transport, such as the second sound effect and various more deviations from Fourier's law in nanoscale systems (Sec. V). In most cases, such novel properties of PnCs stem from static nanopatterns of holes, pillars, or self-assembled nanostructures. An interesting research direction is the synthesis of microscopic, hypersonic PnCs with tunable structures. Tunable hypersonic PnCs

can result from liquid–solid or organic–inorganic heterostructures (Secs. III and VI), which will be controlled by infiltration or deformation, respectively. The waveguiding of phonons (for instance, in a delay line) can be achieved using PnCs with bandgaps and/or topological edge states (Sec. VI). Thus, we consider that research in topological phononics will gradually move to high-order 2D topological nanophononics at gigahertz frequencies.³⁶⁴

ACKNOWLEDGMENTS

This project has received funding from the European Union's Horizon 2020 research and innovation programme (No. 101003436), the Foundation for Polish Science (No. POIR.04.04.00-00-5D1B/18), and the Polish National Science Centre (No. UMO-2018/31/D/ST3/03882).

DATA AVAILABILITY

Data sharing is not applicable to this article as no new data were created or analyzed in this study.

REFERENCES

- ¹J. Frenkel, *Wave Mechanics: Elementary Theory* (Clarendon Press, 1932).
- ²Ig. Tamm, "Über die Quantentheorie der molekularen Lichtzerstreuung in festen Körpern," *Z. Phys.* **60**, 345–363 (1930).
- ³J. M. Ziman, *Electrons and Phonons: The Theory of Transport Phenomena in Solids* (OUP, Oxford, 2001).
- ⁴M. Maldovan, "Sound and heat revolutions in phononics," *Nature* **503**, 209–217 (2013).
- ⁵L. D. Landau, L. P. Pitaevskii, A. M. Kosevich, and E. M. Lifshitz, *Theory of Elasticity*, 3rd ed. (Butterworth-Heinemann, 2012), Vol. 7.
- ⁶B. A. Auld, *Acoustic Fields and Waves in Solids*, 2nd ed. (R. E. Krieger, 1990).
- ⁷P. A. Deymier, *Acoustic Metamaterials and Phononic Crystals* (Springer Science & Business Media, 2013).
- ⁸M. Sledzinska, B. Graczykowski, J. Maire, E. Chavez-Angel, C. M. Sotomayor Torres, and F. Alzina, "2D phononic crystals: Progress and prospects in hypersound and Thermal transport engineering," *Adv. Funct. Mater.* **30**, 1904434 (2020).
- ⁹A. Khelif and A. Adibi, *Phononic Crystals: Fundamentals and Applications* (Springer, 2016).
- ¹⁰V. Laude, *Phononic Crystals: Artificial Crystals for Sonic, Acoustic, and Elastic Waves*, De Gruyter Studies in Mathematical Physics No. Vol. 26 (De Gruyter, 2015).
- ¹¹V. Romero-Garcia and A.-C. Hladky-Hennion, *Fundamentals and Applications of Acoustic Metamaterials: From Seismic to Radio Frequency* (Wiley, 2019).
- ¹²Y. Pennec, J. O. Vasseur, B. Djafari-Rouhani, L. Dobrzański, and P. A. Deymier, "Two-dimensional phononic crystals: Examples and applications," *Surf. Sci. Rep.* **65**, 229–291 (2010).
- ¹³F. Warmuth, M. Wormser, and C. Körner, "Single phase 3D phononic band gap material," *Sci. Rep.* **7**, 3843 (2017).
- ¹⁴F. Lucklum and M. J. Vellekoop, "Bandgap engineering of three-dimensional phononic crystals in a simple cubic lattice," *Appl. Phys. Lett.* **113**, 201902 (2018).
- ¹⁵N. Aravantinos-Zafiris, F. Lucklum, and M. M. Sigalas, "Complete phononic band gaps in the 3D Yablonovite structure with spheres," *Ultrasonics* **110**, 106265 (2021).
- ¹⁶M. M. Sigalas and E. N. Economou, "Elastic and acoustic wave band structure," *J. Sound Vib.* **158**, 377–382 (1992).

- ¹⁷M. S. Kushwaha, P. Halevi, L. Dobrzynski, and B. Djafari-Rouhani, "Acoustic band structure of periodic elastic composites," *Phys. Rev. Lett.* **71**, 2022–2025 (1993).
- ¹⁸D. A. Simons, "Reflection of Rayleigh waves by strips, grooves, and periodic arrays of strips or grooves," *J. Acoust. Soc. Am.* **63**, 1292–1301 (1978).
- ¹⁹N. E. Glass, R. Loudon, and A. A. Maradudin, "Propagation of Rayleigh surface waves across a large-amplitude grating," *Phys. Rev. B* **24**, 6843–6861 (1981).
- ²⁰S. R. Seshadri, "Effect of periodic surface corrugation on the propagation of Rayleigh waves," *J. Acoust. Soc. Am.* **65**, 687–694 (1979).
- ²¹M. Maldovan, "Phonon wave interference and thermal bandgap materials," *Nat. Mater.* **14**, 667–674 (2015).
- ²²R. Martínez-Sala, J. Sancho, J. V. Sánchez, V. Gómez, J. Llinares, and F. Meseguer, "Sound attenuation by sculpture," *Nature* **378**, 241–241 (1995).
- ²³Z. Liu, X. Zhang, Y. Mao, Y. Y. Zhu, Z. Yang, C. T. Chan, and P. Sheng, "Locally resonant sonic materials," *Science* **289**, 1734–1736 (2000).
- ²⁴Y. F. Wang, Y. Z. Wang, B. Wu, W. Chen, and Y. S. Wang, "Tunable and active phononic crystals and metamaterials," *Appl. Mech. Rev.* **72**, 040801 (2020).
- ²⁵G. Ma and P. Sheng, "Acoustic metamaterials: From local resonances to broad horizons," *Sci. Adv.* **2**, e1501595 (2016).
- ²⁶H. Ge, M. Yang, C. Ma, M.-H. Lu, Y.-F. Chen, N. Fang, and P. Sheng, "Breaking the barriers: Advances in acoustic functional materials," *Nat. Sci. Rev.* **5**, 159–182 (2018).
- ²⁷S. A. Cummer, J. Christensen, and A. Alù, "Controlling sound with acoustic metamaterials," *Nat. Rev. Mater.* **1**, 16001 (2016).
- ²⁸K. Bertoldi, V. Vitelli, J. Christensen, and M. van Hecke, "Flexible mechanical metamaterials," *Nat. Rev. Mater.* **2**, 17066 (2017).
- ²⁹*Phononic Crystals*, edited by A. Khelif and A. Adibi (Springer, New York, 2016).
- ³⁰A. Palermo, S. Krödel, A. Marzani, and C. Daraio, "Engineered metabarrier as shield from seismic surface waves," *Sci. Rep.* **6**, 39356 (2016).
- ³¹S. Brûlé, E. Javelaud, S. Enoch, and S. Guenneau, "Experiments on seismic metamaterials: Molding surface waves," *Phys. Rev. Lett.* **112**, 133901 (2014).
- ³²S. Brûlé, S. Enoch, and S. Guenneau, "Emergence of seismic metamaterials: Current state and future perspectives," *Phys. Lett. A* **384**, 126034 (2020).
- ³³S. Brûlé, E. H. Javelaud, S. Enoch, and S. Guenneau, "Flat lens effect on seismic waves propagation in the subsoil," *Sci. Rep.* **7**, 18066 (2017).
- ³⁴M. Miniaci, A. Krushynska, F. Bosia, and N. M. Pugno, "Large scale mechanical metamaterials as seismic shields," *New J. Phys.* **18**, 083041 (2016).
- ³⁵S. Krödel, N. Thomé, and C. Daraio, "Wide band-gap seismic metastructures," *Extreme Mech. Lett.* **4**, 111–117 (2015).
- ³⁶A. Colombi, P. Roux, S. Guenneau, P. Gueguen, and R. V. Craster, "Forests as a natural seismic metamaterial: Rayleigh wave bandgaps induced by local resonances," *Sci. Rep.* **6**, 19238 (2016).
- ³⁷A. Maurel, J.-J. Marigo, K. Pham, and S. Guenneau, "Conversion of Love waves in a forest of trees," *Phys. Rev. B* **98**, 134311 (2018).
- ³⁸J. Huang, Y. Liu, and Y. Li, "Trees as large-scale natural phononic crystals: Simulation and experimental verification," *Int. Soil Water Conserv. Res.* **7**, 196–202 (2019).
- ³⁹A. Colombi, D. Colquitt, P. Roux, S. Guenneau, and R. V. Craster, "A seismic metamaterial: The resonant metawedge," *Sci. Rep.* **6**, 27717 (2016).
- ⁴⁰H. Meng, N. Bailey, Y. Chen, L. Wang, F. Ciampa, A. Fabro, D. Chronopoulos, and W. Elmadih, "3D rainbow phononic crystals for extended vibration attenuation bands," *Sci. Rep.* **10**, 18989 (2020).
- ⁴¹B. J. Ash, S. R. Worsfold, P. Vukusic, and G. R. Nash, "A highly attenuating and frequency tailorabile annular hole phononic crystal for surface acoustic waves," *Nat. Commun.* **8**, 174 (2017).
- ⁴²M. Ghasemi Baboly, C. M. Reinke, B. A. Griffin, I. El-Kady, and Z. C. Leseman, "Acoustic waveguiding in a silicon carbide phononic crystals at microwave frequencies," *Appl. Phys. Lett.* **112**, 103504 (2018).
- ⁴³Y. Wang, J. Lee, X.-Q. Zheng, Y. Xie, and P. X.-L. Feng, "Hexagonal boron nitride phononic crystal waveguides," *ACS Photonics* **6**, 3225–3232 (2019).
- ⁴⁴S. Krödel and C. Daraio, "Microlattice metamaterials for tailoring ultrasonic transmission with elastoacoustic hybridization," *Phys. Rev. Appl.* **6**, 064005 (2016).
- ⁴⁵J.-C. Hsu and Y.-D. Lin, "Microparticle concentration and separation inside a droplet using phononic-crystal scattered standing surface acoustic waves," *Sens. Actuators A* **300**, 111651 (2019).
- ⁴⁶X.-F. Li, X. Ni, L. Feng, M.-H. Lu, C. He, and Y.-F. Chen, "Tunable unidirectional sound propagation through a sonic-crystal-based acoustic diode," *Phys. Rev. Lett.* **106**, 084301 (2011).
- ⁴⁷E. Kim and J. Yang, "Review: Wave propagation in granular metamaterials," *Funct. Compos. Struct.* **1**, 012002 (2019).
- ⁴⁸A. Vega-Flick, R. A. Duncan, S. P. Wallen, N. Boechler, C. Stelling, M. Retsch, J. J. Alvarado-Gil, K. A. Nelson, and A. A. Maznev, "Vibrational dynamics of a two-dimensional microgranular crystal," *Phys. Rev. B* **96**, 024303 (2017).
- ⁴⁹A. Mehaney and A. M. Ahmed, "Locally resonant phononic crystals at low frequencies based on porous SiC multilayer," *Sci. Rep.* **9**, 14767 (2019).
- ⁵⁰S.-H. Jo, H. Yoon, Y. C. Shin, M. Kim, and B. D. Youn, "Elastic wave localization and harvesting using double defect modes of a phononic crystal," *J. Appl. Phys.* **127**, 164901 (2020).
- ⁵¹A. Mehaney and A. A. S. Hassan, "Evolution of low-frequency phononic band gaps using quasi-periodic/defected phononic crystals," *Mater. Res. Express* **6**, 105801 (2019).
- ⁵²F. Lucklum and M. Vellekoop, "Design and fabrication challenges for millimeter-scale three-dimensional phononic crystals," *Crystals* **7**, 348 (2017).
- ⁵³M. Vaezi, H. Seitz, and S. Yang, "A review on 3D micro-additive manufacturing technologies," *Int. J. Adv. Manuf. Technol.* **67**, 1721–1754 (2013).
- ⁵⁴D. Beli, A. T. Fabro, M. Ruzzene, and J. R. F. Arruda, "Wave attenuation and trapping in 3D printed cantilever-in-mass metamaterials with spatially correlated variability," *Sci. Rep.* **9**, 5617 (2019).
- ⁵⁵I.-C. Lee, N. Jayaprakash, and C.-H. Yang, "Characterization of ceramic phononic crystals prepared with additive manufacturing: Ultrasonic technique and finite element analysis," *Ceram. Int.* **46**, 27550–27560 (2020).
- ⁵⁶Z. Tian and L. Yu, "Rainbow trapping of ultrasonic guided waves in chirped phononic crystal plates," *Sci. Rep.* **7**, 40004 (2017).
- ⁵⁷K. L. Tsakmakidis, A. D. Boardman, and O. Hess, "Trapped rainbow' storage of light in metamaterials," *Nature* **450**, 397–401 (2007).
- ⁵⁸Y. Y. Chen, R. Zhu, M. V. Barnhart, and G. L. Huang, "Enhanced flexural wave sensing by adaptive gradient-index metamaterials," *Sci. Rep.* **6**, 35048 (2016).
- ⁵⁹H. Meng, D. Chronopoulos, A. Fabro, W. Elmadih, and I. Maskery, "Rainbow metamaterials for broadband multi-frequency vibration attenuation: Numerical analysis and experimental validation," *J. Sound Vib.* **465**, 115005 (2020).
- ⁶⁰Z. Zhang, K. G. Demir, and G. X. Gu, "Developments in 4D-printing: A review on current smart materials, technologies, and applications," *Int. J. Smart Nano Mater.* **10**, 205–224 (2019).
- ⁶¹X. K. Han and Z. Zhang, "Topological optimization of phononic crystal thin plate by a genetic algorithm," *Sci. Rep.* **9**, 8331 (2019).
- ⁶²S. Kumar and H. P. Lee, "Recent advances in acoustic metamaterials for simultaneous sound attenuation and air ventilation performances," *Crystals* **10**, 686 (2020).
- ⁶³A. Bacigalupo, G. Gnecco, M. Lepidi, and L. Gambarotta, "Machine-learning techniques for the optimal design of acoustic metamaterials," *J. Optim. Theor. Appl.* **187**, 630–653 (2020).
- ⁶⁴T. Brunet, J. Leng, and O. Mondain-Monval, "Soft acoustic metamaterials," *Science* **342**, 323–324 (2013).
- ⁶⁵J. Pierre, B. Dollet, and V. Leroy, "Resonant acoustic propagation and negative density in liquid foams," *Phys. Rev. Lett.* **112**, 148307 (2014).
- ⁶⁶B. Bonello, L. Belliard, J. Pierre, J. O. Vasseur, B. Perrin, and O. Boyko, "Negative refraction of surface acoustic waves in the subgigahertz range," *Phys. Rev. B* **82**, 104109 (2010).
- ⁶⁷T. Brunet, A. Merlin, B. Mascaro, K. Zimny, J. Leng, O. Poncelet, C. Aristegui, and O. Mondain-Monval, "Soft 3D acoustic metamaterial with negative index," *Nat. Mater.* **14**, 384–388 (2015).

- ⁶⁸L. R. Meza, A. J. Zelhofer, N. Clarke, A. J. Mateos, D. M. Kochmann, and J. R. Greer, "Resilient 3D hierarchical architected metamaterials," *Proc. Natl. Acad. Sci. U.S.A.* **112**, 11502–11507 (2015).
- ⁶⁹D. Jang, L. R. Meza, F. Greer, and J. R. Greer, "Fabrication and deformation of three-dimensional hollow ceramic nanostructures," *Nat. Mater.* **12**, 893–898 (2013).
- ⁷⁰L. R. Meza, S. Das, and J. R. Greer, "Strong, lightweight, and recoverable three-dimensional ceramic nanolattices," *Science* **345**, 1322–1326 (2014).
- ⁷¹R. H. Olsson, III and I. El-Kady, "Microfabricated phononic crystal devices and applications," *Meas. Sci. Technol.* **20**, 012002 (2009).
- ⁷²M. Eidini and G. H. Paulino, "Unraveling metamaterial properties in zigzag-base folded sheets," *Sci. Adv.* **1**, e1500224 (2015).
- ⁷³J. T. Overvelde, T. A. de Jong, Y. Shevchenko, S. A. Becerra, G. M. Whitesides, J. C. Weaver, C. Hoberman, and K. Bertoldi, "A three-dimensional actuated origami-inspired transformable metamaterial with multiple degrees of freedom," *Nat. Commun.* **7**, 10929 (2016).
- ⁷⁴D. M. Sussman, Y. Cho, T. Castle, X. Gong, E. Jung, S. Yang, and R. D. Kamien, "Algorithmic lattice kirigami: A route to pluripotent materials," *Proc. Natl. Acad. Sci. U.S.A.* **112**, 7449–7453 (2015).
- ⁷⁵M. Kadic, T. Bückmann, N. Stenger, M. Thiel, and M. Wegener, "On the practicability of pentamode mechanical metamaterials," *Appl. Phys. Lett.* **100**, 191901 (2012).
- ⁷⁶V. Romero Garcia and A.-C. Hladky-Hennion, *Fundamentals and Applications of Acoustic Metamaterials: From Seismic to Radio Frequency* (Wiley, Hoboken, NJ, 2019).
- ⁷⁷S. Benchabane, O. Gaiffe, R. Salut, G. Ulliac, V. Laude, and K. Kokkonen, "Guidance of surface waves in a micron-scale phononic crystal line-defect waveguide," *Appl. Phys. Lett.* **106**, 081903 (2015).
- ⁷⁸D. Zhang, J. Zhao, B. Bonello, F. Zhang, W. Yuan, Y. Pan, and Z. Zhong, "Investigation of surface acoustic wave propagation in composite pillar based phononic crystals within both local resonance and Bragg scattering mechanism regimes," *J. Phys. D: Appl. Phys.* **50**, 435602 (2017).
- ⁷⁹D. B. Go, M. Z. Atashbar, Z. Ramshani, and H.-C. Chang, "Surface acoustic wave devices for chemical sensing and microfluidics: A review and perspective," *Anal. Methods* **9**, 4112–4134 (2017).
- ⁸⁰L. Y. Yeo and J. R. Friend, "Surface acoustic wave microfluidics," *Annu. Rev. Fluid Mech.* **46**, 379–406 (2014).
- ⁸¹R. J. Shilton, S. M. Langelier, J. R. Friend, and L. Y. Yeo, "Surface acoustic wave solid-state rotational micromotor," *Appl. Phys. Lett.* **100**, 033503 (2012).
- ⁸²M. S. Faiz, M. Addouche, A. R. M. Zain, K. S. Siow, A. Chalalane, and A. Khelif, "Experimental demonstration of multichannel elastic wave filter in a phononic crystal slab," *Appl. Sci.* **10**, 4594 (2020).
- ⁸³M. Ghasemi Baboly, A. Raza, J. Brady, C. M. Reinke, Z. C. Leseman, and I. El-Kady, "Demonstration of acoustic waveguiding and tight bending in phononic crystals," *Appl. Phys. Lett.* **109**, 183504 (2016).
- ⁸⁴G.-S. Liu, Y. Zhou, M.-H. Liu, Y. Yuan, X.-Y. Zou, and J.-C. Cheng, "Acoustic waveguide with virtual soft boundary based on metamaterials," *Sci. Rep.* **10**, 981 (2020).
- ⁸⁵H. Pichard, A. Duclos, J.-P. Groby, V. Tournat, L. Zheng, and V. E. Gusev, "Surface waves in granular phononic crystals," *Phys. Rev. E* **93**, 023008 (2016).
- ⁸⁶M. A. Porter, P. G. Kevrekidis, and C. Daraio, "Granular crystals: Nonlinear dynamics meets materials engineering," *Phys. Today* **68**, 44–50 (2015).
- ⁸⁷G. Theocharis, N. Boechler, and C. Daraio, "Nonlinear periodic phononic structures and granular crystals," in *Acoustic Metamaterials and Phononic Crystals*, Springer Series in Solid-State Sciences, edited by P. A. Deymier (Springer, Berlin, 2013), Vol. 173, pp. 217–251.
- ⁸⁸C. Chong, F. Li, J. Yang, M. O. Williams, I. G. Kevrekidis, P. G. Kevrekidis, and C. Daraio, "Damped-driven granular chains: An ideal playground for dark breathers and multibreathers," *Phys. Rev. E* **89**, 032924 (2014).
- ⁸⁹A. Merkel, V. Tournat, and V. Gusev, "Experimental evidence of rotational elastic waves in granular phononic crystals," *Phys. Rev. Lett.* **107**, 225502 (2011).
- ⁹⁰N. Boechler, G. Theocharis, and C. Daraio, "Bifurcation-based acoustic switching and rectification," *Nat. Mater.* **10**, 665–668 (2011).
- ⁹¹F. Li, P. Anzel, J. Yang, P. G. Kevrekidis, and C. Daraio, "Granular acoustic switches and logic elements," *Nat. Commun.* **5**, 5311 (2014).
- ⁹²N. Boechler, J. K. Eliason, A. Kumar, A. A. Maznev, K. A. Nelson, and N. Fang, "Interaction of a contact resonance of microspheres with surface acoustic waves," *Phys. Rev. Lett.* **111**, 036103 (2013).
- ⁹³A. Khanolkar, S. Wallen, M. Abi Ghanem, J. Jenks, N. Vogel, and N. Boechler, "A self-assembled metamaterial for Lamb waves," *Appl. Phys. Lett.* **107**, 071903 (2015).
- ⁹⁴J. K. Eliason, A. Vega-Flick, M. Hiraiwa, A. Khanolkar, T. Gan, N. Boechler, N. Fang, K. A. Nelson, and A. A. Maznev, "Resonant attenuation of surface acoustic waves by a disordered monolayer of microspheres," *Appl. Phys. Lett.* **108**, 061907 (2016).
- ⁹⁵V. Babacic, J. Varghese, E. Coy, E. Kang, M. Pochylski, J. Gapinski, G. Fytas, and B. Graczykowski, "Mechanical reinforcement of polymer colloidal crystals by supercritical fluids," *J. Colloid Interface Sci.* **579**, 786–793 (2020).
- ⁹⁶H. Kim, Y. Cang, E. Kang, B. Graczykowski, M. Secchi, M. Montagna, R. D. Priestley, E. M. Furst, and G. Fytas, "Direct observation of polymer surface mobility via nanoparticle vibrations," *Nat. Commun.* **9**, 2918 (2018).
- ⁹⁷M. Hiraiwa, M. Abi Ghanem, S. Wallen, A. Khanolkar, A. Maznev, and N. Boechler, "Complex contact-based dynamics of microsphere monolayers revealed by resonant attenuation of surface acoustic waves," *Phys. Rev. Lett.* **116**, 198001 (2016).
- ⁹⁸L. Fan, H. Ge, S.-Y. Zhang, H.-F. Gao, Y.-H. Liu, and H. Zhang, "Nonlinear acoustic fields in acoustic metamaterial based on a cylindrical pipe with periodically arranged side holes," *J. Acoust. Soc. Am.* **133**, 3846–3852 (2013).
- ⁹⁹L. Fan, Z. Chen, Y.-C. Deng, J. Ding, H. Ge, S.-Y. Zhang, Y.-T. Yang, and H. Zhang, "Nonlinear effects in a metamaterial with double negativity," *Appl. Phys. Lett.* **105**, 041904 (2014).
- ¹⁰⁰Z. Chen, C. Xue, L. Fan, S.-Y. Zhang, X.-J. Li, H. Zhang, and J. Ding, "A tunable acoustic metamaterial with double-negativity driven by electromagnets," *Sci. Rep.* **6**, 30254 (2016).
- ¹⁰¹K. J. B. Lee, M. K. Jung, and S. H. Lee, "Highly tunable acoustic metamaterials based on a resonant tubular array," *Phys. Rev. B* **86**, 184302 (2012).
- ¹⁰²P. Wang, F. Casadei, S. Shan, J. C. Weaver, and K. Bertoldi, "Harnessing buckling to design tunable locally resonant acoustic metamaterials," *Phys. Rev. Lett.* **113**, 014301 (2014).
- ¹⁰³J. J. Park, K. J. B. Lee, O. B. Wright, M. K. Jung, and S. H. Lee, "Giant acoustic concentration by extraordinary transmission in zero-mass metamaterials," *Phys. Rev. Lett.* **110**, 244302 (2013).
- ¹⁰⁴Y. Jin, Y. Pennec, Y. Pan, and B. Djafari-Rouhani, "Phononic crystal plate with hollow pillars actively controlled by fluid filling," *Crystals* **6**, 64 (2016).
- ¹⁰⁵Z. Liang, M. Willatzen, J. Li, and J. Christensen, "Tunable acoustic double negativity metamaterial," *Sci. Rep.* **2**, 859 (2012).
- ¹⁰⁶J. Wen, H. Shen, D. Yu, and X. Wen, "Exploration of amphoteric and negative refraction imaging of acoustic sources via active metamaterials," *Phys. Lett. A* **377**, 2199–2206 (2013).
- ¹⁰⁷B.-I. Popa, L. Zogoneanu, and S. A. Cummer, "Tunable active acoustic metamaterials," *Phys. Rev. B* **88**, 024303 (2013).
- ¹⁰⁸S. Xiao, G. Ma, Y. Li, Z. Yang, and P. Sheng, "Active control of membrane-type acoustic metamaterial by electric field," *Appl. Phys. Lett.* **106**, 091904 (2015).
- ¹⁰⁹G. Ma, X. Fan, P. Sheng, and M. Fink, "Shaping reverberating sound fields with an actively tunable metasurface," *Proc. Natl. Acad. Sci. U.S.A.* **115**, 6638–6643 (2018).
- ¹¹⁰X. Chen, X. Xu, S. Ai, H. Chen, Y. Pei, and X. Zhou, "Active acoustic metamaterials with tunable effective mass density by gradient magnetic fields," *Appl. Phys. Lett.* **105**, 071913 (2014).
- ¹¹¹S. Babaee, J. T. B. Overvelde, E. R. Chen, V. Tournat, and K. Bertoldi, "Reconfigurable origami-inspired acoustic waveguides," *Sci. Adv.* **2**, e1601019 (2016).
- ¹¹²T. Bückmann, M. Thiel, M. Kadic, R. Schittny, and M. Wegener, "An elastomechanical unfeelability cloak made of pentamode metamaterials," *Nat. Commun.* **5**, 4130 (2014).

- ¹¹³P. Zhang and A. C. To, "Broadband wave filtering of bioinspired hierarchical phononic crystal," *Appl. Phys. Lett.* **102**, 121910 (2013).
- ¹¹⁴T. Chang, S. Jeon, M. Heo, and J. Shin, "Mimicking bio-mechanical principles in photonic metamaterials for giant broadband nonlinearity," *Commun. Phys.* **3**, 79 (2020).
- ¹¹⁵S. Zhu, X. Tan, B. Wang, S. Chen, J. Hu, L. Ma, and L. Wu, "Bio-inspired multistable metamaterials with reusable large deformation and ultra-high mechanical performance," *Extreme Mech. Lett.* **32**, 100548 (2019).
- ¹¹⁶W. Cheng, J. Wang, U. Jonas, G. Fytas, and N. Stefanou, "Observation and tuning of hypersonic bandgaps in colloidal crystals," *Nat. Mater.* **5**, 830–836 (2006).
- ¹¹⁷G. Zhu, N. Z. Swinteck, S. Wu, J. S. Zhang, H. Pan, J. D. Bass, P. A. Deymier, D. Banerjee, and K. Yano, "Direct observation of the phonon dispersion of a three-dimensional solid/solid hypersonic colloidal crystal," *Phys. Rev. B* **88**, 144307 (2013).
- ¹¹⁸A. S. Salasyuk, A. V. Scherbakov, D. R. Yakovlev, A. V. Akimov, A. A. Kaplyanskii, S. F. Kaplan, S. A. Grudinkin, A. V. Nashchekin, A. B. Pevtsov, V. G. Golubev, T. Berstermann, C. Brüggemann, M. Bombeck, and M. Bayer, "Filtering of elastic waves by opal-based hypersonic crystal," *Nano Lett.* **10**, 1319–1323 (2010).
- ¹¹⁹P. J. Beltram, D. Schneider, G. Fytas, and E. M. Furst, "Anisotropic hypersonic phonon propagation in films of aligned ellipsoids," *Phys. Rev. Lett.* **113**, 205503 (2014).
- ¹²⁰E. Alonso-Redondo, M. Schmitt, Z. Urbach, C. M. Hui, R. Sainidou, P. Rembert, K. Matyjaszewski, M. R. Bockstaller, and G. Fytas, "A new class of tunable hypersonic phononic crystals based on polymer-tethered colloids," *Nat. Commun.* **6**, 8309 (2015).
- ¹²¹B. Graczykowski, N. Vogel, K. Bley, H.-J. Butt, and G. Fytas, "Multiband hypersound filtering in two-dimensional colloidal crystals: Adhesion, resonances, and periodicity," *Nano Lett.* **20**, 1883–1889 (2020).
- ¹²²B. Graczykowski, M. Sledzinska, F. Alzina, J. Gomis-Bresco, J. S. Reparaz, M. R. Wagner, and C. M. Sotomayor Torres, "Phonon dispersion in hypersonic two-dimensional phononic crystal membranes," *Phys. Rev. B* **91**, 075414 (2015).
- ¹²³R. Dehghannasiri, A. A. Eftekhar, and A. Adibi, "Hypersonic surface phononic bandgap demonstration in a CMOS-compatible pillar-based piezoelectric structure on silicon," *Phys. Rev. Appl.* **10**, 064019 (2018).
- ¹²⁴M. R. Wagner, B. Graczykowski, J. S. Reparaz, A. El Sachat, M. Sledzinska, F. Alzina, and C. M. Sotomayor Torres, "Two-dimensional phononic crystals: Disorder matters," *Nano Lett.* **16**, 5661–5668 (2016).
- ¹²⁵G. N. Aliev and B. Goller, "Quasi-periodic fibonacci and periodic one-dimensional hypersonic phononic crystals of porous silicon: Experiment and simulation," *J. Appl. Phys.* **116**, 094903 (2014).
- ¹²⁶B. Graczykowski, M. Sledzinska, N. Kehagias, F. Alzina, J. S. Reparaz, and C. M. Sotomayor Torres, "Hypersonic phonon propagation in one-dimensional surface phononic crystal," *Appl. Phys. Lett.* **104**, 123108 (2014).
- ¹²⁷S. Wu, G. Zhu, J. S. Zhang, D. Banerjee, J. D. Bass, C. Ling, and K. Yano, "Anisotropic lattice expansion of three-dimensional colloidal crystals and its impact on hypersonic phonon band gaps," *Phys. Chem. Chem. Phys.* **16**, 8921 (2014).
- ¹²⁸M. Sledzinska, B. Graczykowski, F. Alzina, J. Santiso Lopez, and C. Sotomayor Torres, "Fabrication of phononic crystals on free-standing silicon membranes," *Microelectron. Eng.* **149**, 41–45 (2016).
- ¹²⁹D. Nardi, M. Travagliati, M. E. Siemens, Q. Li, M. M. Murnane, H. C. Kapteyn, G. Ferrini, F. Parmigiani, and F. Banfi, "Probing thermomechanics at the nanoscale: Impulsively excited pseudosurface acoustic waves in hypersonic phononic crystals," *Nano Lett.* **11**, 4126–4133 (2011).
- ¹³⁰M. Travagliati, D. Nardi, C. Giannetti, V. Gusev, P. Pingue, V. Piazza, G. Ferrini, and F. Banfi, "Interface nano-confined acoustic waves in polymeric surface phononic crystals," *Appl. Phys. Lett.* **106**, 021906 (2015).
- ¹³¹T.-W. Liu, Y.-C. Tsai, Y.-C. Lin, T. Ono, S. Tanaka, and T.-T. Wu, "Design and fabrication of a phononic-crystal-based love wave resonator in GHz range," *AIP Adv.* **4**, 124201 (2014).
- ¹³²D. Yudhistira, A. Boes, B. Graczykowski, F. Alzina, L. Y. Yeo, C. M. Sotomayor Torres, and A. Mitchell, "Nanoscale pillar hypersonic surface phononic crystals," *Phys. Rev. B* **94**, 094304 (2016).
- ¹³³A. M. Rakhytmhanov, A. Gueddida, E. Alonso-Redondo, Z. N. Utlegulov, D. Perevoznik, K. Kurselis, B. N. Chichkov, E. H. El Boudouti, B. Djafari-Rouhani, and G. Fytas, "Band structure of cavity-type hypersonic phononic crystals fabricated by femtosecond laser-induced two-photon polymerization," *Appl. Phys. Lett.* **108**, 201901 (2016).
- ¹³⁴M. Ghasemi Baboly, S. Alaie, C. M. Reinke, I. El-Kady, and Z. C. Leseman, "Ultra-high frequency, high Q/volume micromechanical resonators in a planar AlN phononic crystal," *J. Appl. Phys.* **120**, 034502 (2016).
- ¹³⁵R. Pourabolghasem, R. Dehghannasiri, A. A. Eftekhar, and A. Adibi, "Waveguiding effect in the gigahertz frequency range in pillar-based phononic-crystal slabs," *Phys. Rev. Appl.* **9**, 014013 (2018).
- ¹³⁶C. Y. T. Huang, F. Kargar, T. Debnath, B. Debnath, M. D. Valentini, R. Synowicki, S. Schoeche, R. K. Lake, and A. A. Balandin, "Phononic and photonic properties of shape-engineered silicon nanoscale pillar arrays," *Nanotechnology* **31**, 30LT01 (2020).
- ¹³⁷V. L. Zhang, C. G. Hou, H. H. Pan, F. S. Ma, M. H. Kuok, H. S. Lim, S. C. Ng, M. G. Cottam, M. Jamali, and H. Yang, "Phononic dispersion of a two-dimensional chessboard-patterned bicomponent array on a substrate," *Appl. Phys. Lett.* **101**, 053102 (2012).
- ¹³⁸R. Sainidou, N. Stefanou, and A. Modinos, "Widening of phononic transmission gaps via anderson localization," *Phys. Rev. Lett.* **94**, 205503 (2005).
- ¹³⁹G. Gkantzounis, T. Amoah, and M. Florescu, "Hyperuniform disordered phononic structures," *Phys. Rev. B* **95**, 094120 (2017).
- ¹⁴⁰N. Yazdani, M. Jansen, D. Bozyigit, W. M. M. Lin, S. Volk, O. Yarema, M. Yarema, F. Juranyi, S. D. Huber, and V. Wood, "Nanocrystal superlattices as phonon-engineered solids and acoustic metamaterials," *Nat. Commun.* **10**, 1 (2019).
- ¹⁴¹B. Munkhbat, A. B. Yankovich, D. G. Baranov, R. Verre, E. Olsson, and T. O. Shegai, "Transition metal dichalcogenide metamaterials with atomic precision," *Nat. Commun.* **11**, 4604 (2020).
- ¹⁴²K. S. Novoselov, A. Mishchenko, A. Carvalho, and A. H. C. Neto, "2D materials and van der Waals heterostructures," *Science* **353**, aac9439 (2016).
- ¹⁴³L. C. Parsons and G. T. Andrews, "Brillouin scattering from porous silicon-based optical Bragg mirrors," *J. Appl. Phys.* **111**, 123521 (2012).
- ¹⁴⁴N. D. Lanzillotti-Kimura, A. Fainstein, A. Lemaitre, B. Jusserand, and B. Perrin, "Coherent control of sub-terahertz confined acoustic nanowaves: Theory and experiments," *Phys. Rev. B* **84**, 115453 (2011).
- ¹⁴⁵P. M. Walker, J. S. Sharp, A. V. Akimov, and A. J. Kent, "Coherent elastic waves in a one-dimensional polymer hypersonic crystal," *Appl. Phys. Lett.* **97**, 073106 (2010).
- ¹⁴⁶F. Döring, H. Ulrichs, S. Pagel, M. Müller, M. Mansurova, M. Müller, C. Eberl, T. Erichsen, D. Huebner, P. Vana, K. Mann, M. Münzenberg, and H.-U. Krebs, "Confinement of phonon propagation in laser deposited tungsten/polycarbonate multilayers," *New J. Phys.* **18**, 092002 (2016).
- ¹⁴⁷D. Schneider, F. Liaqat, E. H. El Boudouti, O. El Abouti, W. Tremel, H.-J. Butt, B. Djafari-Rouhani, and G. Fytas, "Defect-controlled hypersound propagation in hybrid superlattices," *Phys. Rev. Lett.* **111**, 164301 (2013).
- ¹⁴⁸N. Gomopoulos, D. Maschke, C. Y. Koh, E. L. Thomas, W. Tremel, H.-J. Butt, and G. Fytas, "One-dimensional hypersonic phononic crystals," *Nano Lett.* **10**, 980–984 (2010).
- ¹⁴⁹Z. Lazcano, O. Meza, and J. Arriaga, "Localization of acoustic modes in periodic porous silicon structures," *Nanoscale Res. Lett.* **9**, 419 (2014).
- ¹⁵⁰G. Arregui, N. Lanzillotti-Kimura, C. Sotomayor-Torres, and P. García, "Anderson photon-phonon colocalization in certain random superlattices," *Phys. Rev. Lett.* **122**, 043903 (2019).
- ¹⁵¹G. Wu, Y. Zhu, S. Merugu, N. Wang, C. Sun, and Y. Gu, "GHz spurious mode free AlN lamb wave resonator with high figure of merit using one dimensional phononic crystal tethers," *Appl. Phys. Lett.* **109**, 013506 (2016).
- ¹⁵²H. Fu, "Colloidal metal halide perovskite nanocrystals: A promising juggernaut in photovoltaic applications," *J. Mater. Chem. A* **7**, 14357–14379 (2019).
- ¹⁵³J. Chang and E. R. Waclawik, "Colloidal semiconductor nanocrystals: Controlled synthesis and surface chemistry in organic media," *RSC Adv.* **4**, 23505–23527 (2014).

- ¹⁵⁴D. V. Talapin, E. V. Shevchenko, A. Kornowski, N. Gaponik, M. Haase, A. L. Rogach, and H. Weller, "A new approach to crystallization of CdSe nanoparticles into ordered three-dimensional superlattices," *Adv. Mater.* **13**, 1868–1871 (2001).
- ¹⁵⁵X.-H. Li, J.-X. Li, G.-D. Li, D.-P. Liu, and J.-S. Chen, "Controlled synthesis, growth mechanism, and properties of monodisperse CdS colloidal spheres," *Chem. Eur. J.* **13**, 8754–8761 (2007).
- ¹⁵⁶M. A. Hines and G. D. Scholes, "Colloidal PbS nanocrystals with size-tunable near-infrared emission: Observation of post-synthesis self-narrowing of the particle size distribution," *Adv. Mater.* **15**, 1844–1849 (2003).
- ¹⁵⁷C. L. Poyer, T. Czerniuk, A. Akimov, B. T. Diroll, E. A. Gaulding, A. S. Salasyuk, A. J. Kent, D. R. Yakovlev, M. Bayer, and C. B. Murray, "Coherent acoustic phonons in colloidal semiconductor nanocrystal superlattices," *ACS Nano* **10**, 1163–1169 (2016).
- ¹⁵⁸A. Mondal, J. Aneesh, V. Kumar Ravi, R. Sharma, W. J. Mir, M. C. Beard, A. Nag, and K. V. Adarsh, "Ultrafast exciton many-body interactions and hot-phonon bottleneck in colloidal cesium lead halide perovskite nanocrystals," *Phys. Rev. B* **98**, 115418 (2018).
- ¹⁵⁹K. Chen, S. Schünemann, and H. Tüysüz, "Preparation of waterproof organometal halide perovskite photonic crystal beads," *Angew. Chem.* **129**, 6648–6652 (2017).
- ¹⁶⁰K. E. Knowles, K. H. Hartstein, T. B. Kilburn, A. Marchioro, H. D. Nelson, P. J. Whitham, and D. R. Gamelin, "Luminescent colloidal semiconductor nanocrystals containing copper: Synthesis, photophysics, and applications," *Chem. Rev.* **116**, 10820–10851 (2016).
- ¹⁶¹S. Schünemann, S. Brittman, K. Chen, E. C. Garnett, and H. Tüysüz, "Halide perovskite 3D photonic crystals for distributed feedback lasers," *ACS Photonics* **4**, 2522–2528 (2017).
- ¹⁶²H. Seiler, S. Palato, C. Sonnichsen, H. Baker, E. Socie, D. P. Strandell, and P. Kambhampati, "Two-dimensional electronic spectroscopy reveals liquid-like lineshape dynamics in CsPbI₃ perovskite nanocrystals," *Nat. Commun.* **10**, 4962 (2019).
- ¹⁶³H. Seiler, S. Palato, and P. Kambhampati, "Investigating exciton structure and dynamics in colloidal CdSe quantum dots with two-dimensional electronic spectroscopy," *J. Chem. Phys.* **149**, 074702 (2018).
- ¹⁶⁴M. Khosla, S. Rao, and S. Gupta, "Polarons explain luminescence behavior of colloidal quantum dots at low temperature," *Sci. Rep.* **8**, 8385 (2018).
- ¹⁶⁵P.-A. Mante, C. C. Stoumpos, M. G. Kanatzidis, and A. Yartsev, "Electron-acoustic phonon coupling in single crystal CH₃NH₃PbI₃ perovskites revealed by coherent acoustic phonons," *Nat. Commun.* **8**, 14398 (2017).
- ¹⁶⁶D. Oron, A. Aharoni, C. de Mello Donega, J. van Rijssel, A. Meijerink, and U. Banin, "Universal role of discrete acoustic phonons in the low-temperature optical emission of colloidal quantum dots," *Phys. Rev. Lett.* **102**, 177402 (2009).
- ¹⁶⁷B. Villa, A. J. Bennett, D. J. P. Ellis, J. P. Lee, J. Skiba-Szymanska, T. A. Mitchell, J. P. Griffiths, I. Farrer, D. A. Ritchie, C. J. B. Ford, and A. J. Shields, "Surface acoustic wave modulation of a coherently driven quantum dot in a pillar microcavity," *Appl. Phys. Lett.* **111**, 011103 (2017).
- ¹⁶⁸P. Delsing, A. N. Cleland, M. J. A. Schuetz, J. Knörzer, G. Giedke, J. I. Cirac, K. Srinivasan, M. Wu, K. C. Balram, C. Bäuerle, T. Meunier, C. J. B. Ford, P. V. Santos, E. Cerdá-Méndez, H. Wang, H. J. Krenner, E. D. S. Nysten, M. Weiß, G. R. Nash, L. Thevenard, C. Gourdon, P. Rovillain, M. Marangolo, J.-Y. Duquesne, G. Fischerauer, W. Ruile, A. Reiner, B. Paschke, D. Denysenko, D. Volkmer, A. Wixforth, H. Bruus, M. Wiklund, J. Reboud, J. M. Cooper, Y. Fu, M. S. Brugger, F. Rehfeldt, and C. Westerhausen, "The 2019 surface acoustic waves roadmap," *J. Phys. D: Appl. Phys.* **52**, 353001 (2019).
- ¹⁶⁹J. Pei, J. Yang, X. Wang, F. Wang, S. Mokkapati, T. Lü, J.-C. Zheng, Q. Qin, D. Neshev, H. H. Tan, C. Jagadish, and Y. Lu, "Excited state biexcitons in atomically thin MoSe₂," *ACS Nano* **11**, 7468–7475 (2017).
- ¹⁷⁰Y. Yang, X. Li, M. Wen, E. Hacopian, W. Chen, Y. Gong, J. Zhang, B. Li, W. Zhou, P. M. Ajayan, Q. Chen, T. Zhu, and J. Lou, "Brittle fracture of 2D MoSe₂," *Adv. Mater.* **29**, 1604201 (2017).
- ¹⁷¹M. Sledzinska, B. Graczykowski, M. Placidi, D. S. Reig, A. E. Sachat, J. S. Reparaz, F. Alzina, B. Mortazavi, R. Quey, L. Colombo, S. Roche, and C. M. S. Torres, "Thermal conductivity of MoS₂ polycrystalline nanomembranes," *2D Mater.* **3**, 035016 (2016).
- ¹⁷²S. Bertolazzi, J. Brivio, and A. Kis, "Stretching and breaking of ultrathin MoS₂," *ACS Nano* **5**, 9703–9709 (2011).
- ¹⁷³X. Zhang, C. De-Eknamkul, J. Gu, A. L. Boehmke, V. M. Menon, J. Khurgin, and E. Cubukcu, "Guiding of visible photons at the Ångström thickness limit," *Nat. Nanotechnol.* **14**, 844–850 (2019).
- ¹⁷⁴V. Nicolosi, M. Chhowalla, M. G. Kanatzidis, M. S. Strano, and J. N. Coleman, "Liquid exfoliation of layered materials," *Science* **340**, 1226419–1226419 (2013).
- ¹⁷⁵H. Li, J. Wu, Z. Yin, and H. Zhang, "Preparation and applications of mechanically exfoliated single-layer and multilayer MoS₂ and WSe₂ nanosheets," *Acc. Chem. Res.* **47**, 1067–1075 (2014).
- ¹⁷⁶T. Yun, H. M. Jin, D. Kim, K. H. Han, G. G. Yang, G. Y. Lee, G. S. Lee, J. Y. Choi, I. Kim, and S. O. Kim, "2D metal chalcogenide nanopatterns by block copolymer lithography," *Adv. Funct. Mater.* **28**, 1804508 (2018).
- ¹⁷⁷J. P. Thiruraman, P. Masih Das, and M. Drndić, "Irradiation of transition metal dichalcogenides using a focused ion beam: Controlled single-atom defect creation," *Adv. Funct. Mater.* **29**, 1904668 (2019).
- ¹⁷⁸R. Kozubek, M. Tripathi, M. Ghorbani-Asl, S. Kretschmer, L. Madauß, E. Pollmann, M. O'Brien, N. McEvoy, U. Ludacka, T. Susi, G. S. Duesberg, R. A. Wilhelm, A. V. Krasheninnikov, J. Kotakoski, and M. Schleberger, "Perforating freestanding molybdenum disulfide monolayers with highly charged ions," *J. Phys. Chem. Lett.* **10**, 904–910 (2019).
- ¹⁷⁹D. S. Fox, Y. Zhou, P. Maguire, A. O'Neill, C. Ó'Coileáin, R. Gatensby, A. M. Glushenkov, T. Tao, G. S. Duesberg, I. V. Shvets, M. Abid, M. Abid, H.-C. Wu, Y. Chen, J. N. Coleman, J. F. Donegan, and H. Zhang, "Nanopatterning and electrical tuning of MoS₂ layers with a subnanometer helium ion beam," *Nano Lett.* **15**, 5307–5313 (2015).
- ¹⁸⁰T. Vasileiadis, H. Zhang, H. Wang, M. Bonn, G. Fytas, and B. Graczykowski, "Frequency-domain study of nonthermal gigahertz phonons reveals fano coupling to charge carriers," *Sci. Adv.* **6**, eabd4540 (2020).
- ¹⁸¹M. Eichenfield, J. Chan, R. M. Camacho, K. J. Vahala, and O. Painter, "Optomechanical crystals," *Nature* **462**, 78–82 (2009).
- ¹⁸²J. Chan, T. M. Alegre, A. H. Safavi-Naeini, J. T. Hill, A. Krause, S. Gröblacher, M. Aspelmeyer, and O. Painter, "Laser cooling of a nanomechanical oscillator into its quantum ground state," *Nature* **478**, 89–92 (2011).
- ¹⁸³K. Fang, M. H. Matheny, X. Luan, and O. Painter, "Optical transduction and routing of microwave phonons in cavity-optomechanical circuits," *Nat. Photonics* **10**, 489–496 (2016).
- ¹⁸⁴D. Navarro-Urrios, N. E. Capuj, J. Gomis-Bresco, F. Alzina, A. Pitanti, A. Grilo, A. Martínez, and C. S. Torres, "A self-stabilized coherent phonon source driven by optical forces," *Sci. Rep.* **5**, 1–7 (2015).
- ¹⁸⁵M. Bagheri, M. Poot, M. Li, W. P. Pernice, and H. X. Tang, "Dynamic manipulation of nanomechanical resonators in the high-amplitude regime and non-volatile mechanical memory operation," *Nat. Nanotechnol.* **6**, 726–732 (2011).
- ¹⁸⁶A. G. Krause, M. Winger, T. D. Blasius, Q. Lin, and O. Painter, "A high-resolution microchip optomechanical accelerometer," *Nat. Photonics* **6**, 768 (2012).
- ¹⁸⁷A. H. Safavi-Naeini, T. M. Alegre, J. Chan, M. Eichenfield, M. Winger, Q. Lin, J. T. Hill, D. E. Chang, and O. Painter, "Electromagnetically induced transparency and slow light with optomechanics," *Nature* **472**, 69–73 (2011).
- ¹⁸⁸V. Peano, C. Brendel, M. Schmidt, and F. Marquardt, "Topological phases of sound and light," *Phys. Rev. X* **5**, 031011 (2015).
- ¹⁸⁹J. Gomis-Bresco, D. Navarro-Urrios, M. Oudich, S. El-Jallal, A. Grilo, D. Puerto, E. Chavez, Y. Pennec, B. Djafari-Rouhani, F. Alzina *et al.*, "A one-dimensional optomechanical crystal with a complete phononic band gap," *Nat. Commun.* **5**, 1–6 (2014).
- ¹⁹⁰A. H. Safavi-Naeini, J. T. Hill, S. Meenehan, J. Chan, S. Gröblacher, and O. Painter, "Two-dimensional phononic-photonic band gap optomechanical crystal cavity," *Phys. Rev. Lett.* **112**, 153603 (2014).

- ¹⁹¹G. Heinrich, M. Ludwig, J. Qian, B. Kubala, and F. Marquardt, "Collective dynamics in optomechanical arrays," *Phys. Rev. Lett.* **107**, 043603 (2011).
- ¹⁹²K. Pelka, V. Peano, and A. Xuereb, "Chimera states in small optomechanical arrays," *Phys. Rev. Res.* **2**, 013201 (2020).
- ¹⁹³M. F. Colombano, G. Arregui, N. E. Capuj, A. Pitanti, J. Maire, A. Griol, B. Garrido, A. Martínez, C. M. Sotomayor-Torres, and D. Navarro-Urrios, "Synchronization of optomechanical nanobeams by mechanical interaction," *Phys. Rev. Lett.* **123**, 017402 (2019).
- ¹⁹⁴M. Zhang, S. Shah, J. Cardenas, and M. Lipson, "Synchronization and phase noise reduction in micromechanical oscillator arrays coupled through light," *Phys. Rev. Lett.* **115**, 163902 (2015).
- ¹⁹⁵J. T. Hill, A. H. Safavi-Naeini, J. Chan, and O. Painter, "Coherent optical wavelength conversion via cavity optomechanics," *Nat. Commun.* **3**, 1–7 (2012).
- ¹⁹⁶R. Singh and T. P. Purdy, "Detecting acoustic blackbody radiation with an optomechanical antenna," *Phys. Rev. Lett.* **125**, 120603 (2020).
- ¹⁹⁷W. Jiang, C. J. Sarabalis, Y. D. Dahmani, R. N. Patel, F. M. Mayor, T. P. McKenna, R. Van Laer, and A. H. Safavi-Naeini, "Efficient bidirectional piezo-optomechanical transduction between microwave and optical frequency," *Nat. Commun.* **11**, 1–7 (2020).
- ¹⁹⁸G. S. MacCabe, H. Ren, J. Luo, J. D. Cohen, H. Zhou, A. Sipahigil, M. Mirhosseini, and O. Painter, "Nano-acoustic resonator with ultralong phonon lifetime," *Science* **370**, 840–843 (2020).
- ¹⁹⁹A. H. Ghadimi, S. A. Fedorov, N. J. Engelsen, M. J. Bereyhi, R. Schilling, D. J. Wilson, and T. J. Kippenberg, "Elastic strain engineering for ultralow mechanical dissipation," *Science* **360**, 764–768 (2018).
- ²⁰⁰H. Ren, T. Shah, H. Pfeifer, C. Brendel, V. Peano, F. Marquardt, and O. Painter, "Topological phonon transport in an optomechanical system," *arXiv:2009.06174* (2020).
- ²⁰¹P. Yu and M. Cardona, *Fundamentals of Semiconductors: Physics and Materials Properties*, 4th ed., Graduate Texts in Physics (Springer-Verlag, 2010).
- ²⁰²D. G. Cahill, W. K. Ford, K. E. Goodson, G. D. Mahan, A. Majumdar, H. J. Maris, R. Merlin, and S. R. Phillpot, "Nanoscale thermal transport," *J. Appl. Phys.* **93**, 793–818 (2003).
- ²⁰³G. Chen, *Nanoscale Energy Transport and Conversion: A Parallel Treatment of Electrons, Molecules, Phonons, and Photons* (Oxford University Press, 2005).
- ²⁰⁴D. G. Cahill, P. V. Braun, G. Chen, D. R. Clarke, S. Fan, K. E. Goodson, P. Kebinski, W. P. King, G. D. Mahan, A. Majumdar, H. J. Maris, S. R. Phillpot, E. Pop, and L. Shi, "Nanoscale thermal transport. II. 2003–2012," *Appl. Phys. Rev.* **1**, 011305 (2014).
- ²⁰⁵S. Volz, J. Ordóñez-Miranda, A. Shchepetov, M. Prunnila, J. Ahopelto, T. Pezeril, G. Vaudel, V. Gusev, P. Ruello, E. M. Weig, M. Schubert, M. Hettich, M. Grossman, T. Dekorsy, F. Alzina, B. Graczykowski, E. Chavez-Angel, J. Sebastian Reparaz, M. R. Wagner, C. M. Sotomayor-Torres, S. Xiong, S. Neogi, and D. Donadio, "Nanophononics: State of the art and perspectives," *Eur. Phys. J. B* **89**, 15 (2016).
- ²⁰⁶J. Lee, W. Lee, G. Wehmeyer, S. Dhuey, D. L. Olynick, S. Cabrini, C. Dames, J. J. Urban, and P. Yang, "Investigation of phonon coherence and backscattering using silicon nanomeshes," *Nat. Commun.* **8**, 14054 (2017).
- ²⁰⁷J.-K. Yu, S. Mitrovic, D. Tham, J. Varghese, and J. R. Heath, "Reduction of thermal conductivity in phononic nanomesh structures," *Nat. Nanotechnol.* **5**, 718–721 (2010).
- ²⁰⁸B. Graczykowski, A. E. Sachat, J. S. Reparaz, M. Sledzinska, M. R. Wagner, E. Chavez-Angel, Y. Wu, S. Volz, Y. Wu, F. Alzina, and C. M. S. Torres, "Thermal conductivity and air-mediated losses in periodic porous silicon membranes at high temperatures," *Nat. Commun.* **8**, 415 (2017).
- ²⁰⁹M. Sledzinska, B. Graczykowski, F. Alzina, U. Melia, K. Termentzidis, D. Lacroix, and C. M. S. Torres, "Thermal conductivity in disordered porous nanomembranes," *Nanotechnology* **30**, 265401 (2019).
- ²¹⁰M. Nomura, J. Nakagawa, Y. Kage, J. Maire, D. Moser, and O. Paul, "Thermal phonon transport in silicon nanowires and two-dimensional phononic crystal nanostructures," *Appl. Phys. Lett.* **106**, 143102 (2015).
- ²¹¹J. Maire, R. Anufriev, R. Yanagisawa, A. Ramiere, S. Volz, and M. Nomura, "Heat conduction tuning by wave nature of phonons," *Sci. Adv.* **3**, e1700027 (2017).
- ²¹²N. Zen, T. A. Puurinen, T. J. Isotalo, S. Chaudhuri, and I. J. Maasilta, "Engineering thermal conductance using a two-dimensional phononic crystal," *Nat. Commun.* **5**, 3435 (2014).
- ²¹³J. Lim, H.-T. Wang, J. Tang, S. C. Andrews, H. So, J. Lee, D. H. Lee, T. P. Russell, and P. Yang, "Simultaneous thermoelectric property measurement and incoherent phonon transport in holey silicon," *ACS Nano* **10**, 124–132 (2016).
- ²¹⁴J. Tang, H.-T. Wang, D. H. Lee, M. Fardy, Z. Huo, T. P. Russell, and P. Yang, "Holey silicon as an efficient thermoelectric material," *Nano Lett.* **10**, 4279–4283 (2010).
- ²¹⁵M. N. Luckyanova, J. Garg, K. Esfarjani, A. Jandl, M. T. Bulsara, A. J. Schmidt, A. J. Minnich, S. Chen, M. S. Dresselhaus, Z. Ren, E. A. Fitzgerald, and G. Chen, "Coherent phonon heat conduction in superlattices," *Science* **338**, 936–939 (2012).
- ²¹⁶M. N. Luckyanova, J. Mendoza, H. Lu, B. Song, S. Huang, J. Zhou, M. Li, Y. Dong, H. Zhou, J. Garlow, L. Wu, B. J. Kirby, A. J. Grutter, A. A. Puretzky, Y. Zhu, M. S. Dresselhaus, A. Gossard, and G. Chen, "Phonon localization in heat conduction," *Sci. Adv.* **4**, eaat9460 (2018).
- ²¹⁷J. Ravichandran, A. K. Yadav, R. Cheaito, P. B. Rossen, A. Soukiasian, S. J. Suresha, J. C. Duda, B. M. Foley, C.-H. Lee, Y. Zhu, A. W. Lichtenberger, J. E. Moore, D. A. Muller, D. G. Schlom, P. E. Hopkins, A. Majumdar, R. Ramesh, and M. A. Zurbuchen, "Crossover from incoherent to coherent phonon scattering in epitaxial oxide superlattices," *Nat. Mater.* **13**, 168–172 (2014).
- ²¹⁸K. Takahashi, M. Fujikane, Y. Liao, M. Kashiwagi, T. Kawasaki, N. Tambo, S. Ju, Y. Naito, and J. Shiomi, "Elastic inhomogeneity and anomalous thermal transport in ultrafine Si phononic crystals," *Nano Energy* **71**, 104581 (2020).
- ²¹⁹M. Kasprzak, M. Sledzinska, K. Zaleski, I. Iatsunskyi, F. Alzina, S. Volz, C. M. Sotomayor Torres, and B. Graczykowski, "High-temperature silicon thermal diode and switch," *Nano Energy* **78**, 105261 (2020).
- ²²⁰N. Tambo, Y. Liao, C. Zhou, E. M. Ashley, K. Takahashi, P. F. Nealey, Y. Naito, and J. Shiomi, "Ultimate suppression of thermal transport in amorphous silicon nitride by phononic nanostructure," *Sci. Adv.* **6**, eabc0075 (2020).
- ²²¹S. Alaike, D. F. Goettler, M. Su, Z. C. Leseman, C. M. Reinke, and I. El-Kady, "Thermal transport in phononic crystals and the observation of coherent phonon scattering at room temperature," *Nat. Commun.* **6**, 7228 (2015).
- ²²²P. E. Hopkins, C. M. Reinke, M. F. Su, R. H. Olsson, E. A. Shaner, Z. C. Leseman, J. R. Serrano, L. M. Phinney, and I. El-Kady, "Reduction in the thermal conductivity of single crystalline silicon by phononic crystal patterning," *Nano Lett.* **11**, 107–112 (2011).
- ²²³G. Xie, D. Ding, and G. Zhang, "Phonon coherence and its effect on thermal conductivity of nanostructures," *Adv. Phys. X* **3**, 1480417 (2018).
- ²²⁴R. Anufriev, A. Ramiere, J. Maire, and M. Nomura, "Heat guiding and focusing using ballistic phonon transport in phononic nanostructures," *Nat. Commun.* **8**, 15505 (2017).
- ²²⁵X. Huang, D. Ohori, R. Yanagisawa, R. Anufriev, S. Samukawa, and M. Nomura, "Coherent and incoherent impacts of nanopillars on the thermal conductivity in silicon nanomembranes," *ACS Appl. Mater. Interfaces* **12**, 25478–25483 (2020).
- ²²⁶W. Chen, D. Talreja, D. Eichfeld, P. Mahale, N. N. Nova, H. Y. Cheng, J. L. Russell, S.-Y. Yu, N. Poilvert, G. Mahan, S. E. Mohney, V. H. Crespi, T. E. Mallouk, J. V. Badding, B. Foley, V. Gopalan, and I. Dabo, "Achieving minimal heat conductivity by ballistic confinement in phononic metalattices," *ACS Nano* **14**, 4235–4243 (2020).
- ²²⁷Q. Hao, D. Xu, H. Zhao, Y. Xiao, and F. J. Medina, "Thermal studies of nanoporous Si films with pitches on the order of 100 nm—Comparison between different pore-drilling techniques," *Sci. Rep.* **8**, 9056 (2018).
- ²²⁸A. Jain, Y.-J. Yu, and A. J. H. McGaughey, "Phonon transport in periodic silicon nanoporous films with feature sizes greater than 100 nm," *Phys. Rev. B* **87**, 195301 (2013).

- ²²⁹N. Jaziri, A. Boughamoura, J. Müller, B. Mezghani, F. Tounsi, and M. Ismail, "A comprehensive review of thermoelectric generators: Technologies and common applications," *Energy Rep.* **6**, 264 (2019).
- ²³⁰D. S. Trimmer, *CRC Handbook of Thermoelectrics* (CRC Press, 1995).
- ²³¹J.-P. Colinge, *Silicon-on-Insulator Technology: Materials to VLSI*, 2nd ed. (Springer US, 1997).
- ²³²A. Sharif, *Harsh Environment Electronics: Interconnect Materials and Performance Assessment* (John Wiley & Sons, 2019).
- ²³³B. L. Davis and M. I. Hussein, "Nanophononic metamaterial: Thermal conductivity reduction by local resonance," *Phys. Rev. Lett.* **112**, 055505 (2014).
- ²³⁴M. I. Hussein, C.-N. Tsai, and H. Honarvar, "Thermal conductivity reduction in a nanophononic metamaterial versus a nanophononic crystal: A review and comparative analysis," *Adv. Funct. Mater.* **30**, 1906718 (2020).
- ²³⁵B. Graczykowski, S. Mielcarek, A. Trzaskowska, J. Sarkar, P. Hakonen, and B. Mroz, "Tuning of a hypersonic surface phononic band gap using a nanoscale two-dimensional lattice of pillars," *Phys. Rev. B* **86**, 085426 (2012).
- ²³⁶X. Huang, S. Gluchko, R. Anufriev, S. Volz, and M. Nomura, "Thermal conductivity reduction in a silicon thin film with nanocones," *ACS Appl. Mater. Interfaces* **11**, 34394–34398 (2019).
- ²³⁷Y. Wu, J. Ordóñez-Miranda, S. Gluchko, R. Anufriev, D. D. S. Meneses, L. D. Campo, S. Volz, and M. Nomura, "Enhanced thermal conduction by surface phonon-polaritons," *Sci. Adv.* **6**, eabb4461 (2020).
- ²³⁸G. E. W. Bauer, E. Saitoh, and B. J. van Wees, "Spin caloritronics," *Nat. Mater.* **11**, 391–399 (2012).
- ²³⁹S. R. Boona, R. C. Myers, and J. P. Heremans, "Spin caloritronics," *Energy Environm. Sci.* **7**, 885–910 (2014).
- ²⁴⁰J. Cunha, T.-L. Guo, G. D. Valle, A. N. Koya, R. P. Zaccaria, and A. Alabastri, "Controlling light, heat, and vibrations in plasmonics and phononics," *Adv. Opt. Mater.* **8**, 2001225 (2020).
- ²⁴¹F. A. Nutz and M. Retsch, "Tailor-made temperature-dependent thermal conductivity via interparticle constriction," *Sci. Adv.* **3**, eaao5238 (2017).
- ²⁴²F. A. Nutz, A. Philipp, B. A. F. Kopera, M. Dulle, and M. Retsch, "Low thermal conductivity through dense particle packings with optimum disorder," *Adv. Mater.* **30**, e1704910 (2018).
- ²⁴³B. Li, L. Wang, and G. Casati, "Thermal diode: Rectification of heat flux," *Phys. Rev. Lett.* **93**, 184301 (2004).
- ²⁴⁴G. Wehmeyer, T. Yabuki, C. Monachon, J. Wu, and C. Dames, "Thermal diodes, regulators, and switches: Physical mechanisms and potential applications," *Appl. Phys. Rev.* **4**, 041304 (2017).
- ²⁴⁵C. Dames, "Solid-state thermal rectification with existing bulk materials," *J. Heat Transfer* **131**, 061301-1–061301-7 (2009).
- ²⁴⁶H. Wang, S. Hu, K. Takahashi, X. Zhang, H. Takamatsu, and J. Chen, "Experimental study of thermal rectification in suspended monolayer graphene," *Nat. Commun.* **8**, 15843 (2017).
- ²⁴⁷D. L. Duong, S. J. Yun, and Y. H. Lee, "van der Waals layered materials: Opportunities and challenges," *ACS Nano* **11**, 11803–11830 (2017).
- ²⁴⁸A. K. Geim and I. V. Grigorieva, "Van der waals heterostructures," *Nature* **499**, 419–425 (2013).
- ²⁴⁹X. Gu, Y. Wei, X. Yin, B. Li, and R. Yang, "Colloquium: Phononic thermal properties of two-dimensional materials," *Rev. Mod. Phys.* **90**, 041002 (2018).
- ²⁵⁰K. V. Klitzing, G. Dorda, and M. Pepper, "New method for high-accuracy determination of the fine-structure constant based on quantized hall resistance," *Phys. Rev. Lett.* **45**, 494–497 (1980).
- ²⁵¹B. A. Bernevig, T. L. Hughes, and S.-C. Zhang, "Quantum spin hall effect and topological phase transition in hgte quantum wells," *Science* **314**, 1757–1761 (2006).
- ²⁵²W. Yao, D. Xiao, and Q. Niu, "Valley-dependent optoelectronics from inversion symmetry breaking," *Phys. Rev. B* **77**, 235406 (2008).
- ²⁵³L. Ju, Z. Shi, N. Nair, Y. Lv, C. Jin, J. Velasco, C. Ojeda-Aristizabal, H. A. Bechtel, M. C. Martin, A. Zettl, J. Analytis, and F. Wang, "Topological valley transport at bilayer graphene domain walls," *Nature* **520**, 650–655 (2015).
- ²⁵⁴J. E. Moore, "The birth of topological insulators," *Nature* **464**, 194–198 (2010).
- ²⁵⁵N. P. Armitage, E. J. Mele, and A. Vishwanath, "Weyl and Dirac semimetals in three-dimensional solids," *Rev. Mod. Phys.* **90**, 015001 (2018).
- ²⁵⁶X. Wan, A. M. Turner, A. Vishwanath, and S. Y. Savrasov, "Topological semi-metal and Fermi-arc surface states in the electronic structure of pyrochlore iridates," *Phys. Rev. B* **83**, 205101 (2011).
- ²⁵⁷H. Weng, C. Fang, Z. Fang, B. A. Bernevig, and X. Dai, "Weyl semimetal phase in noncentrosymmetric transition-metal monophosphides," *Phys. Rev. X* **5**, 011029 (2015).
- ²⁵⁸S.-Y. Xu, C. Liu, S. K. Kushwaha, R. Sankar, J. W. Krizan, I. Belopolski, M. Neupane, G. Bian, N. Alidoust, T.-R. Chang, H.-T. Jeng, C.-Y. Huang, W.-F. Tsai, H. Lin, P. P. Shibayev, F.-C. Chou, R. J. Cava, and M. Z. Hasan, "Observation of Fermi arc surface states in a topological metal," *Science* **347**, 294–298 (2015).
- ²⁵⁹S.-Y. Xu, I. Belopolski, D. S. Sanchez, C. Zhang, G. Chang, C. Guo, G. Bian, Z. Yuan, H. Lu, T.-R. Chang, P. P. Shibayev, M. L. Prokopovych, N. Alidoust, H. Zheng, C.-C. Lee, S.-M. Huang, R. Sankar, F. Chou, C.-H. Hsu, H.-T. Jeng, A. Bansil, T. Neupert, V. N. Strocov, H. Lin, S. Jia, and M. Z. Hasan, "Experimental discovery of a topological Weyl semimetal state in tap," *Sci. Adv.* **1**, e1501092 (2015).
- ²⁶⁰T. Kitagawa, E. Berg, M. Rudner, and E. Demler, "Topological characterization of periodically driven quantum systems," *Phys. Rev. B* **82**, 235114 (2010).
- ²⁶¹N. H. Lindner, G. Refael, and V. Galitski, "Floquet topological insulator in semiconductor quantum wells," *Nat. Phys.* **7**, 490–495 (2011).
- ²⁶²Z. Fang, N. Nagaosa, K. S. Takahashi, A. Asamitsu, R. Mathieu, T. Ogawa, H. Yamada, M. Kawasaki, Y. Tokura, and K. Terakura, "The anomalous hall effect and magnetic monopoles in momentum space," *Science* **302**, 92–95 (2003).
- ²⁶³W. Xi and W. Ku, "Hunting down magnetic monopoles in two-dimensional topological insulators and superconductors," *Phys. Rev. B* **100**, 121201 (2019).
- ²⁶⁴A. Uri, Y. Kim, K. Bagani, C. K. Lewandowski, S. Grover, N. Auerbach, E. O. Lachman, Y. Myasoedov, T. Taniguchi, K. Watanabe, J. Smet, and E. Zeldov, "Nanoscale imaging of equilibrium quantum Hall edge currents and of the magnetic monopole response in graphene," *Nat. Phys.* **16**, 164–170 (2020).
- ²⁶⁵Z. Wang, Y. Chong, J. D. Joannopoulos, and M. Soljačić, "Observation of unidirectional backscattering-immune topological electromagnetic states," *Nature* **461**, 772–775 (2009).
- ²⁶⁶L. Lu, J. D. Joannopoulos, and M. Soljačić, "Topological photonics," *Nat. Photonics* **8**, 821–829 (2014).
- ²⁶⁷T. Ozawa, H. M. Price, A. Amo, N. Goldman, M. Hafezi, L. Lu, M. C. Rechtsman, D. Schuster, J. Simon, O. Zilberberg, and I. Carusotto, "Topological photonics," *Rev. Mod. Phys.* **91**, 015006 (2019).
- ²⁶⁸R. Fleury, D. L. Sounas, C. F. Sieck, M. R. Haberman, and A. Alù, "Sound isolation and giant linear nonreciprocity in a compact acoustic circulator," *Science* **343**, 516–519 (2014).
- ²⁶⁹X. Zhang, M. Xiao, Y. Cheng, M.-H. Lu, and J. Christensen, "Topological sound," *Commun. Phys.* **1**, 97 (2018).
- ²⁷⁰Y. Wu, M. Yang, and P. Sheng, "Perspective: Acoustic metamaterials in transition," *J. Appl. Phys.* **123**, 090901 (2018).
- ²⁷¹Y. Liu, X. Chen, and Y. Xu, "Topological phononics: From fundamental models to real materials," *Adv. Funct. Mater.* **30**, 1904784 (2020).
- ²⁷²R. Resta, "Manifestations of Berry's phase in molecules and condensed matter," *J. Phys.: Condens. Matter* **12**, R107–R143 (2000).
- ²⁷³D. Xiao, M.-C. Chang, and Q. Niu, "Berry phase effects on electronic properties," *Rev. Mod. Phys.* **82**, 1959–2007 (2010).
- ²⁷⁴M. Fruchart and D. Carpentier, "An introduction to topological insulators," *C. R. Phys.* **14**, 779–815 (2013).
- ²⁷⁵D. J. Thouless, M. Kohmoto, M. P. Nightingale, and M. den Nijs, "Quantized hall conductance in a two-dimensional periodic potential," *Phys. Rev. Lett.* **49**, 405–408 (1982).
- ²⁷⁶Z. Zhang, Y. Tian, Y. Cheng, Q. Wei, X. Liu, and J. Christensen, "Topological acoustic delay line," *Phys. Rev. Appl.* **9**, 034032 (2018).
- ²⁷⁷H. Gao, H. Xue, Q. Wang, Z. Gu, T. Liu, J. Zhu, and B. Zhang, "Observation of topological edge states induced solely by non-hermiticity in an acoustic crystal," *Phys. Rev. B* **101**, 180303 (2020).

- ²⁷⁸I. Kim, S. Iwamoto, and Y. Arakawa, "Topologically protected elastic waves in one-dimensional phononic crystals of continuous media," *Appl. Phys. Express* **11**, 017201 (2017).
- ²⁷⁹X. Fan, C. Qiu, Y. Shen, H. He, M. Xiao, M. Ke, and Z. Liu, "Probing Weyl physics with one-dimensional sonic crystals," *Phys. Rev. Lett.* **122**, 136802 (2019).
- ²⁸⁰Z. Zhang, H. Long, C. Liu, C. Shao, Y. Cheng, X. Liu, and J. Christensen, "Deep-subwavelength holey acoustic second-order topological insulators," *Adv. Mater.* **31**, 1904682 (2019).
- ²⁸¹J.-P. Xia, D. Jia, H.-X. Sun, S.-Q. Yuan, Y. Ge, Q.-R. Si, and X.-J. Liu, "Programmable coding acoustic topological insulator," *Adv. Mater.* **30**, 1805002 (2018).
- ²⁸²Z. Tian, C. Shen, J. Li, E. Reit, H. Bachman, J. E. S. Socolar, S. A. Cummer, and T. Jun Huang, "Dispersion tuning and route reconfiguration of acoustic waves in valley topological phononic crystals," *Nat. Commun.* **11**, 762 (2020).
- ²⁸³Z. Zhang, Y. Tian, Y. Wang, S. Gao, Y. Cheng, X. Liu, and J. Christensen, "Directional acoustic antennas based on valley-hall topological insulators," *Adv. Mater.* **30**, 1803229 (2018).
- ²⁸⁴Y.-G. Peng, C.-Z. Qin, D.-G. Zhao, Y.-X. Shen, X.-Y. Xu, M. Bao, H. Jia, and X.-F. Zhu, "Experimental demonstration of anomalous Floquet topological insulator for sound," *Nat. Commun.* **7**, 13368 (2016).
- ²⁸⁵D. Jia, H. Xiang Sun, J. Ping Xia, S. Qi Yuan, X. Jun Liu, and C. Zhang, "Acoustic topological insulator by honeycomb sonic crystals with direct and indirect band gaps," *New J. Phys.* **20**, 093027 (2018).
- ²⁸⁶D. Jia, H. Xiang Sun, S. Qi Yuan, C. Zhang, and X. Jun Liu, "Pseudospin-dependent acoustic topological insulator by airborne sonic crystals with a triangular lattice," *Appl. Phys. Express* **12**, 044003 (2019).
- ²⁸⁷Q. Wei, Y. Tian, S.-Y. Zuo, Y. Cheng, and X.-J. Liu, "Experimental demonstration of topologically protected efficient sound propagation in an acoustic waveguide network," *Phys. Rev. B* **95**, 094305 (2017).
- ²⁸⁸B.-Z. Xia, T.-T. Liu, G.-L. Huang, H.-Q. Dai, J.-R. Jiao, X.-G. Zang, D.-J. Yu, S.-J. Zheng, and J. Liu, "Topological phononic insulator with robust pseudospin-dependent transport," *Phys. Rev. B* **96**, 094106 (2017).
- ²⁸⁹C. He, X. Ni, H. Ge, X.-C. Sun, Y.-B. Chen, M.-H. Lu, X.-P. Liu, and Y.-F. Chen, "Acoustic topological insulator and robust one-way sound transport," *Nat. Phys.* **12**, 1124–1129 (2016).
- ²⁹⁰Z. Zhang, Y. Tian, Y. Cheng, X. Liu, and J. Christensen, "Experimental verification of acoustic pseudospin multipoles in a symmetry-broken snowflakelike topological insulator," *Phys. Rev. B* **96**, 241306 (2017).
- ²⁹¹Y. Deng, H. Ge, Y. Tian, M. Lu, and Y. Jing, "Observation of zone folding induced acoustic topological insulators and the role of spin-mixing defects," *Phys. Rev. B* **96**, 184305 (2017).
- ²⁹²H. Dai, M. Qian, J. Jiao, B. Xia, and D. Yu, "Subwavelength acoustic topological edge states realized by zone folding and the role of boundaries selection," *J. Appl. Phys.* **124**, 175107 (2018).
- ²⁹³Q. Zhang, Y. Chen, K. Zhang, and G. Hu, "Dirac degeneracy and elastic topological valley modes induced by local resonant states," *Phys. Rev. B* **101**, 014101 (2020).
- ²⁹⁴S.-Y. Huo, J.-J. Chen, H.-B. Huang, and G.-L. Huang, "Simultaneous multi-band valley-protected topological edge states of shear vertical wave in two-dimensional phononic crystals with veins," *Sci. Rep.* **7**, 10335 (2017).
- ²⁹⁵H. Xue, Y. Yang, F. Gao, Y. Chong, and B. Zhang, "Acoustic higher-order topological insulator on a kagome lattice," *Nat. Mater.* **18**, 108–112 (2019).
- ²⁹⁶B. Xie, H. Liu, H. Cheng, Z. Liu, S. Chen, and J. Tian, "Acoustic topological transport and refraction in a Kekulé lattice," *Phys. Rev. Appl.* **11**, 044086 (2019).
- ²⁹⁷B.-Z. Xia, S.-J. Zheng, T.-T. Liu, J.-R. Jiao, N. Chen, H.-Q. Dai, D.-J. Yu, and J. Liu, "Observation of valleylike edge states of sound at a momentum away from the high-symmetry points," *Phys. Rev. B* **97**, 155124 (2018).
- ²⁹⁸Z. Zhu, X. Huang, J. Lu, M. Yan, F. Li, W. Deng, and Z. Liu, "Negative refraction and partition in acoustic valley materials of a square lattice," *Phys. Rev. Appl.* **12**, 024007 (2019).
- ²⁹⁹Z. Yang, F. Gao, and B. Zhang, "Topological water wave states in a one-dimensional structure," *Sci. Rep.* **6**, 29202 (2016).
- ³⁰⁰P. Delplace, J. B. Marston, and A. Venaille, "Topological origin of equatorial waves," *Science* **358**, 1075–1077 (2017).
- ³⁰¹N. Laforge, V. Laude, F. Chollet, A. Khelif, M. Kadic, Y. Guo, and R. Fleury, "Observation of topological gravity-capillary waves in a water wave crystal," *New J. Phys.* **21**, 083031 (2019).
- ³⁰²M. P. Makwana, N. Laforge, R. V. Craster, G. Dupont, S. Guenneau, V. Laude, and M. Kadic, "Experimental observations of topologically guided water waves within non-hexagonal structures," *Appl. Phys. Lett.* **116**, 131603 (2020).
- ³⁰³C. He, S.-Y. Yu, H. Ge, H. Wang, Y. Tian, H. Zhang, X.-C. Sun, Y. B. Chen, J. Zhou, M.-H. Lu, and Y.-F. Chen, "Three-dimensional topological acoustic crystals with pseudospin-valley coupled saddle surface states," *Nat. Commun.* **9**, 4555 (2018).
- ³⁰⁴C. He, H.-S. Lai, B. He, S.-Y. Yu, X. Xu, M.-H. Lu, and Y.-F. Chen, "Acoustic analogues of three-dimensional topological insulators," *Nat. Commun.* **11**, 2318 (2020).
- ³⁰⁵H. He, C. Qiu, L. Ye, X. Cai, X. Fan, M. Ke, F. Zhang, and Z. Liu, "Topological negative refraction of surface acoustic waves in a Weyl phononic crystal," *Nature* **560**, 61–64 (2018).
- ³⁰⁶Y. Qi, C. Qiu, M. Xiao, H. He, M. Ke, and Z. Liu, "Acoustic realization of quadrupole topological insulators," *Phys. Rev. Lett.* **124**, 206601 (2020).
- ³⁰⁷X. Ni, M. Li, M. Weiner, A. Alù, and A. B. Khanikaev, "Demonstration of a quantized acoustic octupole topological insulator," *Nat. Commun.* **11**, 2108 (2020).
- ³⁰⁸H. Xue, Y. Ge, H.-X. Sun, Q. Wang, D. Jia, Y.-J. Guan, S.-Q. Yuan, Y. Chong, and B. Zhang, "Observation of an acoustic octupole topological insulator," *Nat. Commun.* **11**, 2442 (2020).
- ³⁰⁹A. Merkel and J. Christensen, "Ultrasonic nodal chains in topological granular metamaterials," *Commun. Phys.* **2**, 154 (2019).
- ³¹⁰Y.-G. Peng, Y. Li, Y.-X. Shen, Z.-G. Geng, J. Zhu, C.-W. Qiu, and X.-F. Zhu, "Chirality-assisted three-dimensional acoustic floquet lattices," *Phys. Rev. Res.* **1**, 033149 (2019).
- ³¹¹Y. Fu, C. Shen, X. Zhu, J. Li, Y. Liu, S. A. Cummer, and Y. Xu, "Sound vortex diffraction via topological charge in phase gradient metagratings," *Sci. Adv.* **6**, eaba9876 (2020).
- ³¹²X. Zhu, K. Li, P. Zhang, J. Zhu, J. Zhang, C. Tian, and S. Liu, "Implementation of dispersion-free slow acoustic wave propagation and phase engineering with helical-structured metamaterials," *Nat. Commun.* **7**, 11731 (2016).
- ³¹³H. Xue, Y. Yang, G. Liu, F. Gao, Y. Chong, and B. Zhang, "Realization of an acoustic third-order topological insulator," *Phys. Rev. Lett.* **122**, 244301 (2019).
- ³¹⁴A. Song, J. Li, C. Shen, T. Chen, and S. A. Cummer, "Switchable directional sound emission with improved field confinement based on topological insulators," *Appl. Phys. Lett.* **117**, 043503 (2020).
- ³¹⁵M. Makwana, R. Craster, and S. Guenneau, "Topological beam-splitting in photonic crystals," *Opt. Express* **27**, 16088–16102 (2019).
- ³¹⁶Y. Tang, Y. Zhu, B. Liang, J. Yang, J. Yang, and J. Cheng, "One-way acoustic beam splitter," *Sci. Rep.* **8**, 13573 (2018).
- ³¹⁷T. Liu, G. Ma, S. Liang, H. Gao, Z. Gu, S. An, and J. Zhu, "Single-sided acoustic beam splitting based on parity-time symmetry," *Phys. Rev. B* **102**, 014306 (2020).
- ³¹⁸M. P. Makwana and G. Chaplain, "Tunable three-way topological energy-splitter," *Sci. Rep.* **9**, 18939 (2019).
- ³¹⁹P. Wang, L. Lu, and K. Bertoldi, "Topological phononic crystals with one-way elastic edge waves," *Phys. Rev. Lett.* **115**, 104302 (2015).
- ³²⁰J. Lu, C. Qiu, L. Ye, X. Fan, M. Ke, F. Zhang, and Z. Liu, "Observation of topological valley transport of sound in sonic crystals," *Nat. Phys.* **13**, 369–374 (2017).
- ³²¹Y. Ding, Y. Peng, Y. Zhu, X. Fan, J. Yang, B. Liang, X. Zhu, X. Wan, and J. Cheng, "Experimental demonstration of acoustic chern insulators," *Phys. Rev. Lett.* **122**, 014302 (2019).
- ³²²Y. Huang, X. Wang, X. Gong, H. Wu, D. Zhang, and D. Zhang, "Contact nonlinear acoustic diode," *Sci. Rep.* **10**, 2564 (2020).

- ³²³J. Zhu, X. Zhu, X. Yin, Y. Wang, and X. Zhang, "Unidirectional extraordinary sound transmission with mode-selective resonant materials," *Phys. Rev. Appl.* **13**, 041001 (2020).
- ³²⁴M. Wang, W. Zhou, L. Bi, C. Qiu, M. Ke, and Z. Liu, "Valley-locked wave-guide transport in acoustic heterostructures," *Nat. Commun.* **11**, 3000 (2020).
- ³²⁵R. Ganesh and S. Gonella, "From modal mixing to tunable functional switches in nonlinear phononic crystals," *Phys. Rev. Lett.* **114**, 054302 (2015).
- ³²⁶M. S. Rudner and N. H. Lindner, "Band structure engineering and non-equilibrium dynamics in Floquet topological insulators," *Nat. Rev. Phys.* **2**, 229–244 (2020).
- ³²⁷S. Li, D. Zhao, H. Niu, X. Zhu, and J. Zang, "Observation of elastic topological states in soft materials," *Nat. Commun.* **9**, 1370 (2018).
- ³²⁸M. Esmann, F. R. Lamberti, A. Lemaître, and N. D. Lanzillotti-Kimura, "Topological acoustics in coupled nanocavity arrays," *Phys. Rev. B* **98**, 161109 (2018).
- ³²⁹M. Esmann, F. R. Lamberti, P. Senellart, I. Favero, O. Krebs, L. Lanço, C. Gomez Carbonell, A. Lemaître, and N. D. Lanzillotti-Kimura, "Topological nanophononic states by band inversion," *Phys. Rev. B* **97**, 155422 (2018).
- ³³⁰G. Arregui, O. Ortíz, M. Esmann, C. M. Sotomayor-Torres, C. Gomez-Carbonell, O. Mauguin, B. Perrin, A. Lemaître, P. D. García, and N. D. Lanzillotti-Kimura, "Coherent generation and detection of acoustic phonons in topological nanocavities," *APL Photonics* **4**, 030805 (2019).
- ³³¹S. Yves, R. Fleury, F. Lemoult, M. Fink, and G. Lerosey, "Topological acoustic polaritons: Robust sound manipulation at the subwavelength scale," *New J. Phys.* **19**, 075003 (2017).
- ³³²S. Anguiano, A. E. Bruchhausen, B. Jusserand, I. Favero, F. R. Lamberti, L. Lanço, I. Sagnes, A. Lemaître, N. D. Lanzillotti-Kimura, P. Senellart, and A. Fainstein, "Micropillar resonators for optomechanics in the extremely high 19–95-GHz frequency range," *Phys. Rev. Lett.* **118**, 263901 (2017).
- ³³³F. R. Lamberti, Q. Yao, L. Lanço, D. T. Nguyen, M. Esmann, A. Fainstein, P. Sesin, S. Anguiano, V. V. ne, A. Bruchhausen, P. Senellart, I. Favero, and N. D. Lanzillotti-Kimura, "Optomechanical properties of gaas/alas micropillar resonators operating in the 18 ghz range," *Opt. Express* **25**, 24437–24447 (2017).
- ³³⁴W. Wang, Y. Jin, W. Wang, B. Bonello, B. Djafari-Rouhani, and R. Fleury, "Robust fano resonance in a topological mechanical beam," *Phys. Rev. B* **101**, 024101 (2020).
- ³³⁵W. Wang, B. Bonello, B. Djafari-Rouhani, and Y. Pennec, "Topological valley, pseudospin, and pseudospin-valley protected edge states in symmetric pillared phononic crystals," *Phys. Rev. B* **100**, 140101 (2019).
- ³³⁶W. Wang, B. Bonello, B. Djafari-Rouhani, and Y. Pennec, "Polarization-dependent and valley-protected Lamb waves in asymmetric pillared phononic crystals," *J. Phys. D: Appl. Phys.* **52**, 505302 (2019).
- ³³⁷P. Ruello and V. E. Gusev, "Physical mechanisms of coherent acoustic phonons generation by ultrafast laser action," *Ultrasonics* **56**, 21–35 (2015).
- ³³⁸B. Graczykowski, A. Guedida, B. Djafari-Rouhani, H.-J. Butt, and G. Fytas, "Brillouin light scattering under one-dimensional confinement: Symmetry and interference self-canceling," *Phys. Rev. B* **99**, 165431 (2019).
- ³³⁹B. Graczykowski, M. Sledzinska, M. Placidi, D. Saleta Reig, M. Kasprzak, F. Alzina, and C. M. Sotomayor Torres, "Elastic properties of few nanometers thick polycrystalline MoS₂ membranes: A nondestructive study," *Nano Lett.* **17**, 7647–7651 (2017).
- ³⁴⁰T. Marchesi D'Alvise, S. Harvey, L. Hueske, J. Szelwicka, L. Veith, T. P. J. Knowles, D. Kubiczek, C. Flraig, F. Port, K.-E. Gottschalk, F. Rosenau, B. Graczykowski, G. Fytas, F. S. Ruggeri, K. Wunderlich, and T. Weil, "Ultrathin polydopamine films with phospholipid nanodiscs containing a glycophorin a domain," *Adv. Funct. Mater.* **30**, 2000378 (2020).
- ³⁴¹Y. Xu, X. Tian, and C. Chen, "Band structures of two dimensional solid/air hierarchical phononic crystals," *Physica B* **407**, 1995–2001 (2012).
- ³⁴²K. Hur, R. G. Hennig, and U. Wiesner, "Exploring periodic bicontinuous cubic network structures with complete phononic bandgaps," *J. Phys. Chem. C* **121**, 22347–22352 (2017).
- ³⁴³C.-Y. Lee, M. J. Leamy, and J. H. Nadler, "Frequency band structure and absorption predictions for multi-periodic acoustic composites," *J. Sound Vib.* **329**, 1809–1822 (2010).
- ³⁴⁴M. I. Hussein, K. Hamza, G. M. Hulbert, and K. Saitou, "Optimal synthesis of 2D phononic crystals for broadband frequency isolation," *Waves Random Complex Media* **17**, 491–510 (2007).
- ³⁴⁵Y. F. Li, X. Huang, F. Meng, and S. Zhou, "Evolutionary topological design for phononic band gap crystals," *Struct. Multidiscipl. Optim.* **54**, 595–617 (2016).
- ³⁴⁶Z.-X. Xu, H. Gao, Y.-J. Ding, J. Yang, B. Liang, and J.-C. Cheng, "Topology-optimized omnidirectional broadband acoustic ventilation barrier," *Phys. Rev. Appl.* **14**, 054016 (2020).
- ³⁴⁷S. M. Sadat and R. Y. Wang, "A machine learning based approach for phononic crystal property discovery," *J. Appl. Phys.* **128**, 025106 (2020).
- ³⁴⁸C. Choi, S. Bansal, N. Münenrieder, and S. Subramanian, "Fabricating and assembling acoustic metamaterials and phononic crystals," *Adv. Eng. Mater.* **23**, 2000988 (2021).
- ³⁴⁹X. Wang, X. Luo, B. Yang, and Z. Huang, "Ultrathin and durable open meta-materials for simultaneous ventilation and sound reduction," *Appl. Phys. Lett.* **115**, 171902 (2019).
- ³⁵⁰T. Delpero, S. Schoenwald, A. Zemp, and A. Bergamini, "Structural engineering of three-dimensional phononic crystals," *J. Sound Vib.* **363**, 156–165 (2016).
- ³⁵¹Y. Ge, H.-X. Sun, S.-Q. Yuan, and Y. Lai, "Switchable omnidirectional acoustic insulation through open window structures with ultrathin metasurfaces," *Phys. Rev. Mater.* **3**, 065203 (2019).
- ³⁵²Y. Ge, H.-X. Sun, S.-Q. Yuan, and Y. Lai, "Broadband unidirectional and omnidirectional bidirectional acoustic insulation through an open window structure with a metasurface of ultrathin hooklike meta-atoms," *Appl. Phys. Lett.* **112**, 243502 (2018).
- ³⁵³P. Wang, T.-N. Chen, K.-P. Yu, and X.-P. Wang, "Lamb wave band gaps in a double-sided phononic plate," *J. Appl. Phys.* **113**, 053509 (2013).
- ³⁵⁴A.-L. Song, T.-N. Chen, X.-P. Wang, and L.-L. Wan, "Waveform-preserved unidirectional acoustic transmission based on impedance-matched acoustic metasurface and phononic crystal," *J. Appl. Phys.* **120**, 085106 (2016).
- ³⁵⁵Y. Xiao, J. Wen, L. Huang, and X. Wen, "Analysis and experimental realization of locally resonant phononic plates carrying a periodic array of beam-like resonators," *J. Phys. D: Appl. Phys.* **47**, 045307 (2013).
- ³⁵⁶L. Li, X. Gang, Z. Sun, X. Zhang, and F. Zhang, "Design of phononic crystals plate and application in vehicle sound insulation," *Adv. Eng. Softw.* **125**, 19–26 (2018).
- ³⁵⁷H. Ryoo and W. Jeon, "Dual-frequency sound-absorbing metasurface based on visco-thermal effects with frequency dependence," *J. Appl. Phys.* **123**, 115110 (2018).
- ³⁵⁸M. Duan, C. Yu, Z. Xu, F. Xin, and T. J. Lu, "Acoustic impedance regulation of Helmholtz resonators for perfect sound absorption via roughened embedded necks," *Appl. Phys. Lett.* **117**, 151904 (2020).
- ³⁵⁹R. Ghaffarivardavagh, J. Nikoliczky, S. Anderson, and X. Zhang, "Ultra-open acoustic metamaterial silencer based on fano-like interference," *Phys. Rev. B* **99**, 024302 (2019).
- ³⁶⁰R. Martinez-Sala, C. Rubio, L. M. Garcia-Raffi, J. V. Sanchez-Perez, E. A. Sanchez-Perez, and J. Llinares, "Control of noise by trees arranged like sonic crystals," *J. Sound Vib.* **291**, 100–106 (2006).
- ³⁶¹S. Zou, Y. Xu, R. Zatianina, C. Li, X. Liang, L. Zhu, Y. Zhang, G. Liu, Q. H. Liu, H. Chen, and Z. Wang, "Broadband waveguide cloak for water waves," *Phys. Rev. Lett.* **123**, 074501 (2019).
- ³⁶²C. Li, L. Xu, L. Zhu, S. Zou, Q. H. Liu, Z. Wang, and H. Chen, "Concentrators for water waves," *Phys. Rev. Lett.* **121**, 104501 (2018).
- ³⁶³T. Kodama, M. Ohnishi, W. Park, T. Shiga, J. Park, T. Shimada, H. Shinohara, J. Shiomi, and K. E. Goodson, "Modulation of thermal and thermoelectric transport in individual carbon nanotubes by fullerene encapsulation," *Nat. Mater.* **16**, 892–897 (2017).
- ³⁶⁴X. Xi, J. Ma, S. Wan, C.-H. Dong, and X. Sun, "Observation of chiral edge states in gapped nanomechanical graphene," *Sci. Adv.* **7**, eabe1398 (2021).